

1 **Dangerous degree forecast of soil and water loss on highway slopes in**
2 **mountainous areas using the revised universal soil and water loss**
3 **equation**

4 **Yue Li^{1,2}, Shi Qi^{*1,2}, Bin Liang^{1,2}, Junming Ma^{1,2}, Baihan Cheng^{1,2}, Cong Ma³, Yidan Qiu³,**
5 **and Qinyan Chen³**

6 ¹ Key Laboratory of State Forestry Administration on Soil and Water Conservation, Beijing
7 Forestry University, Beijing 100083, China

8 ² Beijing Engineering Research Center of Soil and Water Conservation, Beijing Forestry
9 University, Beijing 100083, China

10 ³ Yunnan Science Research Institute of Communication & Transportation, Kunming 650011,
11 China

12

13 **Abstract**

14 Many high and steep slopes are formed by special topographic and geomorphic types and
15 mining activities during the construction of mountain expressways. Severe soil erosion may also
16 occur under heavy rainfall conditions. Therefore, predicting **soil loss** on highway slopes is
17 important in protecting infrastructure and human life. In this study, we investigate Xinhe
18 Expressway located at the southern edge of the Yunnan–Guizhou Plateau. The revised universal
19 soil loss equation is used as the prediction model for soil and water loss on slopes. Geographic
20 information systems, remote sensing technology, field surveys, runoff plot observation testing,
21 cluster analysis and co-kriging calculations are also utilised. The partition of the prediction units
22 of **soil loss** on the expressway slope in the mountainous area and the spatial distribution of rainfall
23 on a linear highway are studied. Given the particularity of the expressway slope in the
24 mountainous area, the model parameter is modified, and the risk of **soil loss** along the mountain
25 expressway is simulated and predicted under 20- and 1-year rainfall return periods. The following
26 results are obtained. (1) Natural watersheds can be considered for the prediction of slope soil
27 erosion to represent the actual situation of **soil loss** on each slope. Then, the spatial location of the
28 soil erosion unit can be determined. (2) Analysis of actual observation data shows that the overall
29 average absolute error of the monitoring area is $33.24 \text{ t}\cdot\text{km}^{-2}\cdot\text{a}^{-1}$, the overall average relative error
30 is 33.96% and the overall root mean square error is between 20.95 and 65.64, all of which are
31 within acceptable limits. The Nash efficiency coefficient is 0.67, indicating that the prediction
32 accuracy of the model satisfies the requirements. (3) Under the 1-year rainfall return period
33 condition, we find through risk classification that the percentage of prediction units with no risk of
34 erosion is 78%. The soil erosion risk is low and does not affect road traffic safety. Under the 20-
35 year return period rainfall condition, the percentage of units with high and extremely high risks is

36 7.11%. The prediction results can help adjust the design of water and soil conservation measures
37 for these units.

38 **Keywords:** Soil loss; highway slopes; mountainous areas; RUSLE; dangerous degree forecast

39

40 **Introduction**

41 China has gradually accelerated its construction of highways in recent years, improved its
42 transportation networks and promoted rapid economic development (Jia et al., 2005). With the
43 implementation of the Western development strategy, advanced requirements for the construction
44 of expressways have been proposed to connect coastal plains and inland mountains. However,
45 many unstable high and steep slopes, such as natural, excavation and fill slopes, are inevitably
46 formed by the frequent filling and deep digging along expressways in mountain areas.

47 The slope is the most fragile part of an expressway in a mountain area. During rainy seasons,
48 soil erosion is easily caused by rainwash and leads to considerable damage (Figure 1). At present,
49 China's highway industry remains in a period of rapid development. At the end of 2014, the total
50 mileage of highway networks exceeded 4,400,000 km, whilst that of expressways was 112,000 km
51 (Yuan et al., 2017; Mori et al., 2017; Kateb et al., 2013; Zhou et al., 2016). Statistics further
52 indicate that in the next 20–30 years, the expressways in China will have a total length of more
53 than 40,000 km. For every kilometre of highway, the corresponding bare slope area is expected to
54 reach 50,000–70,000 m² (Wang, 2006). The annual amount of soil erosion is 9,000 g/m³, which
55 can cause 450 t of soil loss annually (Chen, 2010). The soil loss of roadbed slopes differs from the
56 soil loss in woodlands and farmlands. Forestlands and farmlands are generally formed after years
57 of evolution and belong to the native landscape. Most of the slopes of these land types are gentle
58 and stable (Kateb et al., 2013). Moreover, traditional soil and water conservation research has
59 focused on slopes with 20% grade or below, but roadbed slopes of highways generally have a
60 grade of 30% or above (Zhou, 2010). Soil erosion on roadbed side slopes affects not only soil loss
61 along highways but also road operation safety (Gong and Yang, 2016; Jiang et al., 2017).
62 Therefore, soil erosion on the side slopes of mountain expressways must be studied to control soil
63 erosion, improve the ecological environment of expressways and realise sustainable land
64 utilisation (Wang et al., 2005; Yang and Wang, 2006).

65 The revised universal soil loss equation (RUSLE) is a set of mathematical equations used to
66 estimate the average annual soil loss and sediment yield resulting from inter-rill and rill erosion
67 (Renard et al., 1997; Foster et al., 1999; Zerihun et al., 2018; Toy et al., 2002). RUSLE was
68 derived from the theory of erosion processes and has been applied to more than 10,000 plot-years
69 of data from natural rainfall plots and numerous rainfall-simulation plots. RUSLE is an
70 exceptionally well-validated and documented equation. It was conceptualised by a group of
71 nationally recognised scientists and soil conservationists with extensive experience in erosion

72 processes (Soil and Water Conservation Society, 1993).

73 The use of RUSLE models as predictive tools for the quantitative estimation of soil erosion
74 has matured (Panagos et al., 2018; Cunha et al., 2017; Taye et al., 2017; Renard, 1997). The range
75 of application of these models involves nearly every aspect of soil erosion. Moreover, many
76 scientists have conducted useful explorations to modify the model's parametric values and
77 improve its simulation accuracy.

78 Tresch et al. (1995), in a study in Switzerland, argued that slope length (L) and slope
79 steepness (S) are crucial factors in soil erosion prediction, and these parameters significantly
80 influence the erosion values calculated by RUSLE. All existing S factors can be derived only from
81 gentle slope inclinations of up to 32%; however, many cultivated areas are steeper than this
82 critical value. A previous study used 18 plot measurements on transects along slopes with
83 steepness from 20% to 90% to qualitatively assess the most suitable S factors for steep subalpine
84 slopes; the results showed that the first selection of the S factor is possible for slopes beyond the
85 critical steepness of 25% (Tresch et al., 1995). Rick et al. (2001) found that using universal soil
86 loss equation (USLE) and RUSLE soil erosion models at regional landscape scales is limited by
87 the difficulty of obtaining an LS factor grid suitable for geographic information system (GIS)
88 applications. Therefore, their modifications were applied to the previous arc macro language
89 (AML) code to produce a RUSLE-based version of the LS factor grid. These alterations included
90 replacing the USLE algorithms with their RUSLE counterparts and redefining the assumptions on
91 slope characteristics. In areas of western USA where the models were tested, the RUSLE-based
92 AML program produced LS values that were roughly comparable to those listed in the RUSLE
93 handbook guidelines (Rick et al., 2001). Silburn (2011) showed that estimating the soil erodibility
94 factor (K) from soil properties (derived from cultivated soils) provides a reasonable estimate of K
95 for the main duplex soils at the study site as long as the correction for undisturbed soil is used to
96 derive K from the measured data before application to the USLE model (Silburn, 2011). Wu (2014)
97 adopted GIS and RUSLE methods to analyse the risk pattern of soil erosion in the affected road
98 zone of Hangjinqi Highway in Zhuji City, Zhejiang Province. Digital elevation model (DEM)
99 data, rainfall records, soil type data, remote sensing imaging and a road map of Hangjinqi
100 Highway were used for GIS and RUSLE analyses (Wu et al., 2014). Chen (2010), who initially
101 considered the terrain characteristics of roadbed side slopes and conducted a concrete analysis of
102 the terrain factor calculation method in RUSLE, evaluated a compatible terrain factor
103 computational method of roadbed side slopes and proposed a revised method based on the
104 measured data of soil erosion in the subgrade side slope of Hurongxi Expressway (from Enshi to
105 Lichuan) in Hubei Province. The results indicated that (1) the slope length factor in RUSLE can

106 be calculated by $L = \left(\frac{\lambda}{22.1}\right)^m$, but m should not be computed by using the original method for
107 highway subgrade side slope because its gradient surpasses the generally applicable scope of
108 RUSLE. Moreover, (2) the slope length factor (L) of the highway subgrade side slope can be

109 calculated by $L = \left(\lambda/22.1\right)^{0.35}$ (Chen et al., 2010). Zhang (2016) investigated the spatiotemporal
110 distribution of soil erosion in a ring expressway before and after construction by using a land
111 use/cover map of Ningbo City in 2010. The topographic map of the North Ring Expressway and
112 field survey data were collected for the DEM. Rainfall data were also collected from local
113 hydrological stations. On the basis of the collected data, the spatial distribution of the factors in
114 the RUSLE model was calculated, and soil erosion maps of the North Ring Expressway were
115 estimated. Then, the soil erosion amount was calculated at three different stages by RUSLE. The
116 results showed that slight erosion was dominant during the preconstruction and natural recovery
117 periods, which accounted for 98.53% and 99.73%, respectively. During the construction period,
118 mild erosion and slight erosion had the largest values and accounted for 52.5% and 35.4%,
119 respectively. Soil erosion during the construction period was mainly distributed in temporary
120 ground soil (Zhang et al., 2016).

121 However, the common methods used to fit the parameters can affect the findings, and
122 minimising the sum of the squares of errors for soil loss may provide better results than simply
123 fitting an exponential equation. Yang (2014) found that the *C* factor, as a function of fractional
124 bare soil and ground cover, can be derived from MODIS data at regional or catchment scales. The
125 method offered a meaningful estimate of the *C* factor for determining ground cover impact on soil
126 loss and erosion hazard areas. The method performed better than commonly used techniques based
127 on green vegetation only (e.g. normalised difference vegetation index (NDVI)), and it was
128 appropriate for estimating the vegetation cover management factor (*C*) in the modelled hillslope
129 erosion in New South Wales, Australia by using emerging fractional vegetation cover products.
130 Moreover, the approach effectively mapped the spatiotemporal distribution of the RUSLE cover
131 factor and the hillslope erosion hazard in a large area. The methods and results described in this
132 previous work are important in understanding the spatiotemporal dynamics of hillslope erosion
133 and ground cover. According to Kinnell (2014), runoff production, which is spatially uniform, is
134 often inappropriate under natural conditions because infiltration is spatially variable. Upslope
135 length varies with the ratio of the upslope runoff coefficient to the runoff coefficient for the area
136 below the downslope boundary of the segment in the modified RUSLE approach. The use of
137 upslope length produces only minor variations in soil loss compared with using values predicted
138 by the standard RUSLE approach when the runoff is spatially variable and the number of
139 segments increases. By contrast, the USLE-M approach can predict soil loss that is influenced
140 strongly by runoff when runoff varies in space and time. Therefore, an increase in runoff through a
141 segment causes an increase in soil loss, and a decrease in runoff through a segment or cell results
142 in a decrease in soil loss.

143 In general, past studies (e.g. Tresch et al., 1995; Rick et al., 2001; Silburn, 2011; Yang, 2014;
144 Kinnell, 2014) focused on sloping fields, but the research on soil erosion on highway slopes is
145 limited. Subgrade slope is a major part of soil erosion during construction and operation periods.

146 Therefore, soil erosion caused by subgrade slope should be predicted. However, the research on
147 **soil loss** of highways hardly meets the requirements of practical work (Xu et al., 2009; Bakr et al.,
148 2012). We still need to conduct considerable work on the prediction of soil erosion on highway
149 slopes. The situation in various regions in China indicates that researchers have helped improve
150 the RUSLE model and studied soil erosion in certain areas. Water and soil erosion caused by
151 engineering construction is an important aspect of research, especially from the perspective of
152 agricultural cultivation and forestry deforestation, because the amount of eroded soil produced by
153 embankment slopes accounts for a large proportion of the entire project area. Although this
154 concern is related to project feasibility and cost in particular, the topic has elicited considerable
155 interest in general. Furthermore, the principal factor that causes soil erosion on slopes generally
156 corresponds to precipitation amount and embankment width. Wang (2005) established several
157 experimental standardised spots for soil loss collection on the side slopes of the Xiaogan–Xiang
158 Fan Freeway (i.e. under construction thus far) and installed an on-the-spot rainfall auto-recorder.
159 The collected data were used for the revision of the main parameters R (rainfall and runoff) and K
160 (erodibility of soil) of USLE, which is widely applied to forecast soil loss quantity in plowlands
161 and predict the soil loss quantities of different types of soil on side slopes disturbed by engineering
162 treatments (Wang et al., 2005). This method not only applies to the prediction of disturbed soil
163 loss during expressway construction but also improves prediction accuracy. It also provides
164 scientific support for relevant units or personnel to implement reasonable preventive measures.

165 Related literature indicates that research on **soil loss** in highways has the following
166 limitations. First, most of the studies on C and P factors that used the RUSLE model were
167 conducted by referring to previous research results, and data accuracy is often poor. Second, most
168 studies on rainfall erosivity (R) factors are limited to sloping fields, and the rainfall erosivity
169 factors of expressway slopes in mountain areas have rarely been studied. Third, slope soils in
170 highways differ depending on soil arability, and the slopes also vary. Thus, accurately predicting
171 the soil loss of different types of subgrade slopes by using the traditional K factor calculation
172 method is difficult.

173 Previous studies have shown that the spatial interpolation method of precipitation is
174 unsuitable for the study of the spatiotemporal distribution of precipitation in mountain areas (Liu
175 and Zhang, 2006). The problem involves two aspects. From the timescale perspective, the
176 characteristics of rainfall distribution and the influencing factors are not fully considered. From
177 the spatial scale perspective, the spatial heterogeneity of the region is ignored. Furthermore, many
178 studies have limited the factors that affect precipitation to altitude factors, leading to low
179 interpolation accuracy (Zhao et al., 2011; Liu et al., 2010). Thus, in this study, we consider the
180 spatial heterogeneity of linear engineering of the expressway. The rainfall factor is spatially
181 interpolated to compensate for the following limitations: shortage of rainfall data on mountain
182 areas, difficulty of representing the rainfall data of an entire expressway by using data from a
183 single meteorological station, and uneven spatial distribution and strong heterogeneity of rainfall

184 in mountain areas (Li et al., 2017). We analyse the characteristics of soil erosion to improve
185 certain aspects of expressway construction on the basis of previous research. We divide a highway
186 slope into natural and artificial units and calculate the amount of soil loss from the slope surface to
187 the pavement based on the slope surface catchment unit. The findings can be popularised because
188 this approach is in line with the actual situation. Next, we modify the parameters of the artificial
189 slope through an actual survey, runoff plot observation and other methods, and the parameters of
190 the artificial slope are corrected by referring to the form of the project and the utilised materials.
191 We not only scientifically predict the amount of soil erosion caused by highway construction in
192 mountain areas but also provide a scientific basis for the prevention and control of soil erosion and
193 rational allocation of prevention and control measures. The safe operation of highways and the
194 virtuous cycle of the ecological environment should be ensured to promote the sustainable
195 development of the local economy.

196 **1 Study area**

197 Xinhe Expressway is in the southern margin of the Yunnan–Guizhou Plateau, which is in
198 southeast Yunnan Province, Honghe Prefecture and Hekou County. This highway was the first in
199 Yunnan to cross the border. Thus, it has become an important communication channel between
200 China and Vietnam and possesses an important strategic and economic value. The highway is at
201 longitude $103^{\circ} 33' 45''$ – $103^{\circ} 58' 32''$ and latitude $22^{\circ} 31' 19''$ – $22^{\circ} 51' 48''$ (Figure 2) The
202 expressway stretches roughly from northwest to southeast, and its total length is 56.30 km. The
203 climate type belongs to subtropical mountain, seasonal monsoon forest and humid heat climate
204 categories. Between May and the middle of October, the area experiences wet season
205 characterised by abundant rainfall, concentrated precipitation and increased rain at night time; the
206 variation of precipitation is 400–2000 mm, whilst most regions have 800–1800 mm (Fei et al.,
207 2017; Zhang et al., 2017). During the rest of the year, the area undergoes dry season. The starting
208 point of Xinhe Expressway is in Hekou County, New Street (pile number K83+500), at an altitude
209 of 296 m. The endpoint is in the estuary of Areca Village (pile number K139+800) at an altitude of
210 95 m. The mountains along both sides are 200–380 m above sea level. The topography of the hilly
211 area in the northern part of Xinhe Expressway is complicated. The slopes on both sides rise and
212 fall, and most of the valleys constitute V- and U-shaped sections. The natural slopes on both sides
213 are mostly below 30° . The southern part of the highway has a relatively flat terrain and a gentle
214 slope. The slopes of most hills on both sides are less than 15° , and the overall height difference is
215 less than 100 m. The vegetation in the southern part of Xinhe Expressway includes tropical
216 rainforests and tropical monsoon forests, whilst that in the northern part of China is classified as
217 south subtropical monsoon evergreen broad-leaved forest. In recent years, the original vegetation
218 in this area has been reclaimed as farmland and is now planted with rubber, banana, pineapple and
219 pomegranate, which are sporadic tropical rainforest survivors. The project area along Xinhe
220 Expressway is an economic forest belt with a single vegetation type and mainly has rubber, forest

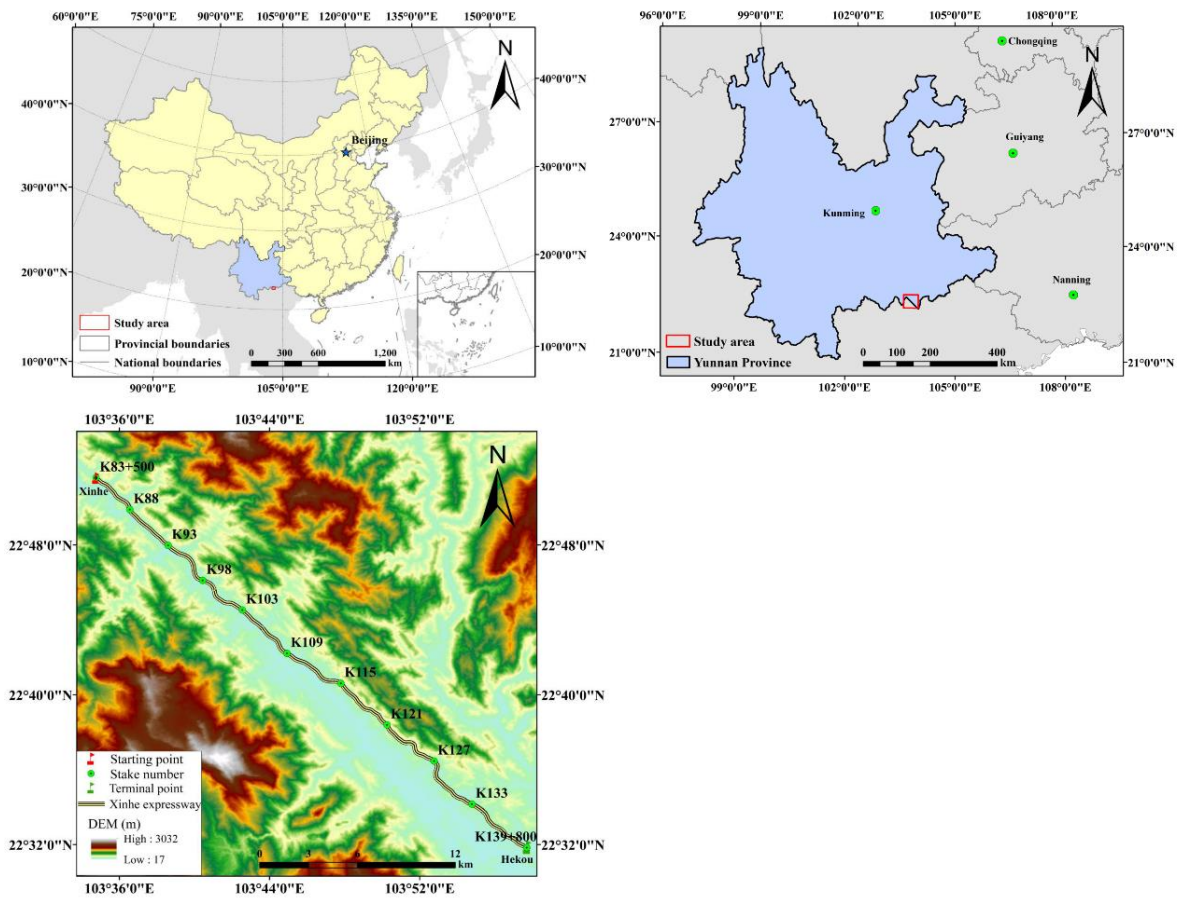
221 and other economic trees. The soil types along the highway are rich and mainly comprise red,
222 leached cinnamon, grey forest and grey cinnamon soils.



223

224

Figure 1. Soil erosion produced by rainwash on a slope after rainfall



225

226

Figure 2. The location and the overview of the study region

227 2 Materials and methods

228 2.1 Data sources

229 Rainfall data from 2014 were obtained from Hekou Yao Autonomous County, Pingbian Miao
230 Autonomous County, Jinping Miao Yao Autonomous County and the meteorological department
231 of Mengzi. The rainfall data were obtained at 5 min intervals. Meanwhile, two automatic weather
232 stations were established along Xinhe Expressway to gather weather data during the 2014
233 experiment. Meteorological data, which were provided by the China Meteorological Data
234 Network, covered the period of 1959–2015 (<http://data.cma.cn/site/index.html>).

235 Data on soil types were provided by Yunnan Traffic Planning and Design Institute. Data on
236 soil texture and organic matter were obtained via field surveys, data sampling and processing
237 methods. Soil samples were initially collected at each 1 km range of the artificial and natural
238 slopes on both sides of the highway. Five mixed soil samples were obtained from one slope by
239 using the ‘S’-shaped sampling method (Shu et al., 2017). Then, the method of coning and
240 quartering was adopted (Oyekanle et al., 2011), and half of the mixed soil samples were brought
241 to the laboratory for analysis. Finally, 186 soil samples were obtained. After the soil samples were
242 dried and sieved, soil texture and organic carbon content were measured via specific gravity speed
243 measurement and potassium dichromate external heating, respectively.

244 The topographic map and design drawings of Xinhe Expressway were provided by the
245 Traffic Planning and Design Institute of Yunnan Province. The 1:2000 scale of the topographic
246 map coordinate system was based on the 2000 GeKaiMeng urban coordinate system, the elevation
247 system for 1985 national height data and the format for the CAD map in DWG. The remote
248 sensing images used in this study were derived from 8 m hyperspectral images produced by the
249 GF-1 satellite (<http://www.rscloudmart.com/>).

250

251 2.2 Prediction model selection

252 The RUSLE equation (Renard et al., 1997) was used to predict soil and water loss on the side
253 slopes of Xinhe Expressway. The RUSLE equation considers natural and anthropogenic factors
254 that cause soil erosion to produce comprehensive results. The parameters are easy to calculate, and
255 the calculation method is relatively mature. The RUSLE model is suitable for soil erosion
256 prediction in areas where physical models are not required. Formula (1) is expressed as

$$257 \quad A = R \cdot K \cdot L \cdot S \cdot C \cdot P, \quad (1)$$

258 where A is the average soil loss per unit area by erosion ($t/ha^2 \cdot y$), R is the rainfall erosivity factor
259 ($MJ \cdot mm / (ha^2 \cdot h \cdot y)$), K is the soil erodibility factor ($t \cdot ha^2 \cdot h / (ha^2 \cdot MJ \cdot mm)$), L is the slope length
260 factor, S is the steepness factor, C is the cover and management practice factor and P is the

261 conservation support practice factor. The values of L , S , C and P are dimensionless.

262

263 2.3 Division and implementation of the prediction unit

264 Geological structures and rock and soil categories are complex because of considerable
265 changes in topography and physiognomy. The forms of slopes also vary. In general, according to
266 the relationship between slope and engineering, slopes can be natural or artificial. Artificial slope
267 formations can be subdivided into slope embankments and cutting slopes. In this study, we used
268 ArcGIS software to convert the topographic map of the highway design into a vectorisation file
269 because the artificial and natural slopes of watershed catchments are the main components of soil
270 erosion prediction. On the basis of the extracted graphical units, the natural and artificial slopes
271 were divided into uniform prediction units according to aspect, slope, land use and water
272 conservation measures. The aspect, slope, land use, water conservation measures and other
273 attributes of each prediction unit were consistent.

274

275 3 Results and analysis

276 3.1 Natural slope catchment area

277 The catchment unit of the slope was initially constructed by using the structural plane tools of
278 ArcGIS combined with ridge and valley lines and artificial slope and highway boundaries
279 (Zerihun et al., 2018). After the completion of the catchment unit, the slope was divided according
280 to soil type data (Table 1). After the division and overlaying of the remote sensing image map, the
281 land use types and soil and water conservation measures were considered as indicators for the
282 visual interpretation of the field survey results and for further classification of the confluence units.
283 The partition units were amended by using the vegetation coverage data obtained along Xinhe
284 Expressway. A total of 814 natural slope catchment prediction units were divided.

285

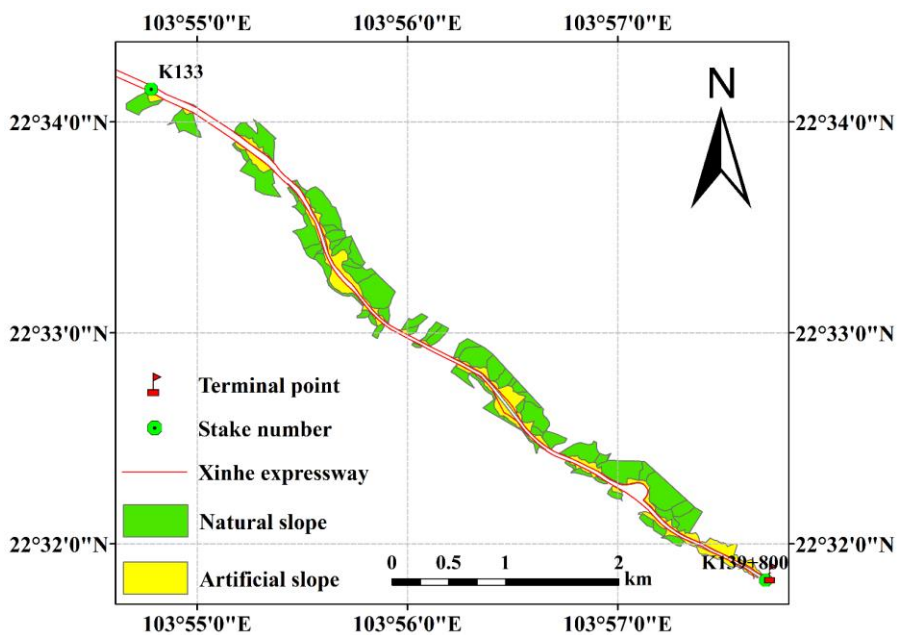
Table 1. Distribution of soil types along Xinhe Expressway

Section of the expressway	Soil type
K83+500~K84+900	latosolic red soil
K85+200~K93+200	leached cinnamon soil
K93+200~K95+900	grey forest soil
K96+900~K97+800	grey cinnamon soil

K97+800~K100+500	leached cinnamon soil
K100+500~K101+100	grey cinnamon soil
K101+100~K104	leached cinnamon soil
K104~K109+100	grey cinnamon soil
K109+100~K139	leached cinnamon soil

286

287 The artificial slope was divided into roadbed and cutting slopes according to the design of
 288 Xinhe Expressway (i.e. 1:1.5 and 1:1.0 slopes). After the preliminary division, the slope
 289 measurements, data design and field survey results were used as a basis for the subsequent
 290 detailed division of the artificial slope into cement frame protection and six arris brick revetments.
 291 McCool (1987) stated that slope length can vary within a 10 m range and only has a small effect
 292 on results. The specifications of each frame in the cement frame protection along Xinhe
 293 Expressway were the same. The horizontal projection length of a cement frame can be regarded
 294 the slope length value of an artificial slope. Therefore, the slope length of the artificial slope of
 295 each frame of the cement revetment was considered the same, and the value was set to 0.
 296 According to investigations, the vegetation coverage of artificial slopes with different plant
 297 species varies substantially. To achieve an accurate prediction of unit division and improve
 298 prediction accuracy, the artificial slopes should be continuously classified according to plant
 299 species. Thus, 422 artificial slope prediction units were obtained. The data of the 1236 slope
 300 prediction units were edited by using GIS. The results are shown in Figure 3.



301

302

Figure 3. Division results of the prediction units (A subset-6.8 km)

303 3.2 Determination of conventional parameters of the RUSLE model

304 3.2.1 Rainfall erosivity factor (R) (Panagos et al., 2017)

305 The formula of the R -value (rainfall erosivity) was adopted (Wang et al., 1995; Liu et al.,
306 1999; Yang et al., 1999) and calculated by using 30 min rainfall intensity as the measure, as shown
307 in Formulas (2) and (3).

308
$$R = 1.70 \cdot (P \cdot I_{30} / 100) - 0.136 \quad (I_{30} < 10 \text{ mm/h}), \quad (2)$$

309
$$R = 2.35 \cdot (P \cdot I_{30} / 100) - 0.523 \quad (I_{30} \geq 10 \text{ mm/h}), \quad (3)$$

310 where R is rainfall erosivity ($\text{MJ} \cdot \text{mm} / (\text{hm}^2 \cdot \text{h})$), P is sub-rainfall (mm) and I_{30} is the maximum 30
311 min rainfall intensity ($\text{mm} \cdot \text{h}^{-1}$).

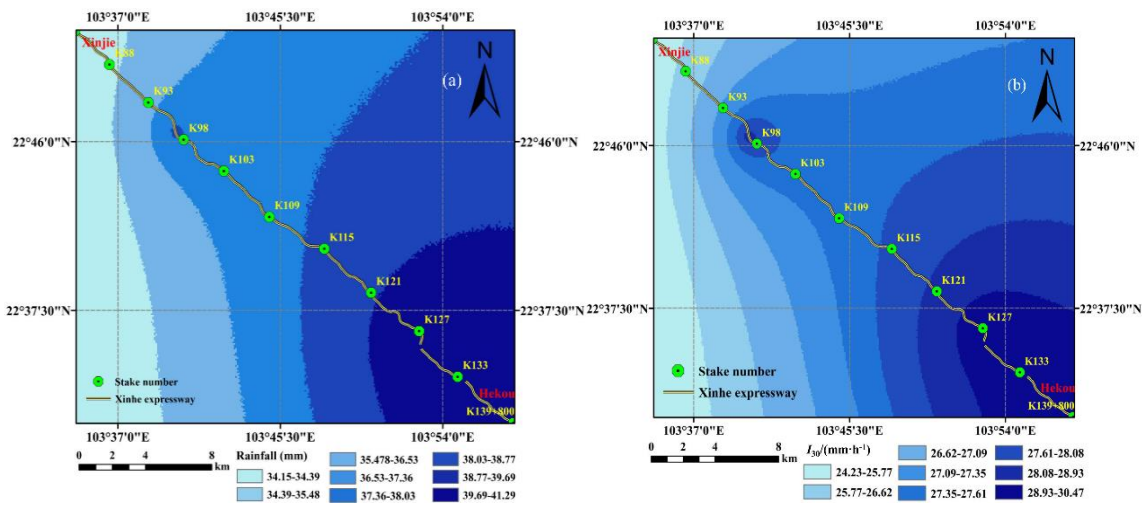
312 Rainfall data were acquired from stationary ground meteorological stations. However, using
313 data from a single meteorological station to represent the rainfall data of a linear mountain
314 expressway is difficult. The P and I_{30} values along the highway were obtained by co-kriging
315 calculations. The dataset included the following: rainfall data; 30 min rainfall data from the four
316 meteorological stations in Hekou Yao Autonomous County, Pingbian Miao Autonomous County,
317 Jinping Miao Yao Autonomous County and Mengzi City; and data acquired from two automatic
318 weather stations along the highway. Then, the cross-validation method was used to evaluate the
319 accuracy of the interpolation results. The selection criteria included the standard root mean square
320 error and the mean standard error. The detailed results are shown in Table 2. However, this work
321 shows only the interpolated results of secondary rainfall of two rainfall events and the 30 min
322 rainfall intensity data, as shown in Figures 4(a) and 4(b).

323 **Table 2.** Interpolation error of P and I_{30} values

Time of the second rainfall	P		I_{30}	
	RMSS	MS	RMSS	MS
2014.06.05	1.02	-0.02	1.06	-0.05
2014.06.07	1.04	-0.02	1.01	0.02
2014.06.17	1.09	0.03	1.11	0.06
2014.06.28	1.11	0.07	1.05	-0.03
2014.07.01	1.10	0.04	1.06	-0.04
2014.07.13	1.03	-0.02	1.01	0.02

2014.07.20	1.01	0.01	1.05	0.02
2014.08.02	1.03	0.03	0.94	0.02
2014.08.12	1.05	-0.03	1.10	0.03
2014.08.26	1.03	0.01	0.97	0.03
2014.08.29	1.09	-0.02	1.03	-0.02
2014.09.02	1.07	0.03	1.05	0.02
2014.09.04	0.96	-0.02	0.97	-0.02
2014.09.17	1.07	-0.03	1.09	-0.03
2014.09.20	0.98	0.05	1.03	0.02
2014.10.05	1.02	0.03	1.04	0.03

324



325

326

Figure 4(a). Interpolation results of secondary rainfall for June 5, 2014

327

Figure 4(b). Interpolation results of I_{30} for June 5, 2014

328

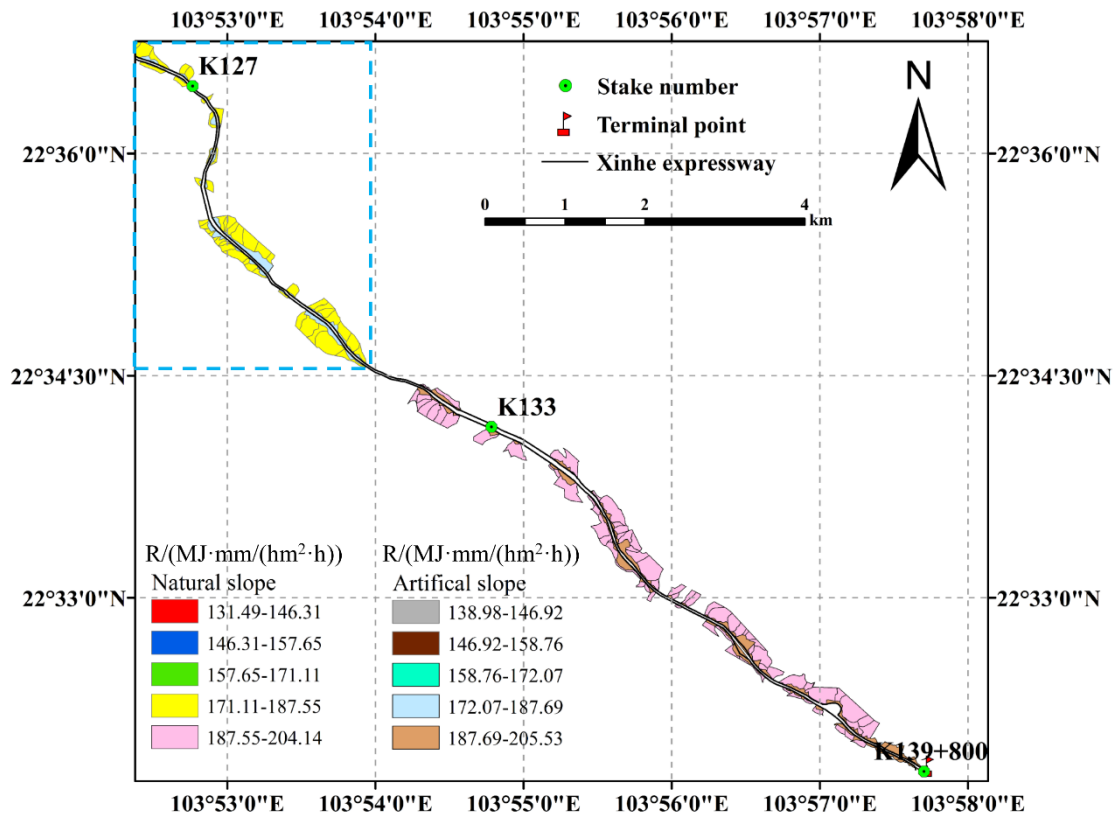
329

330

331

332

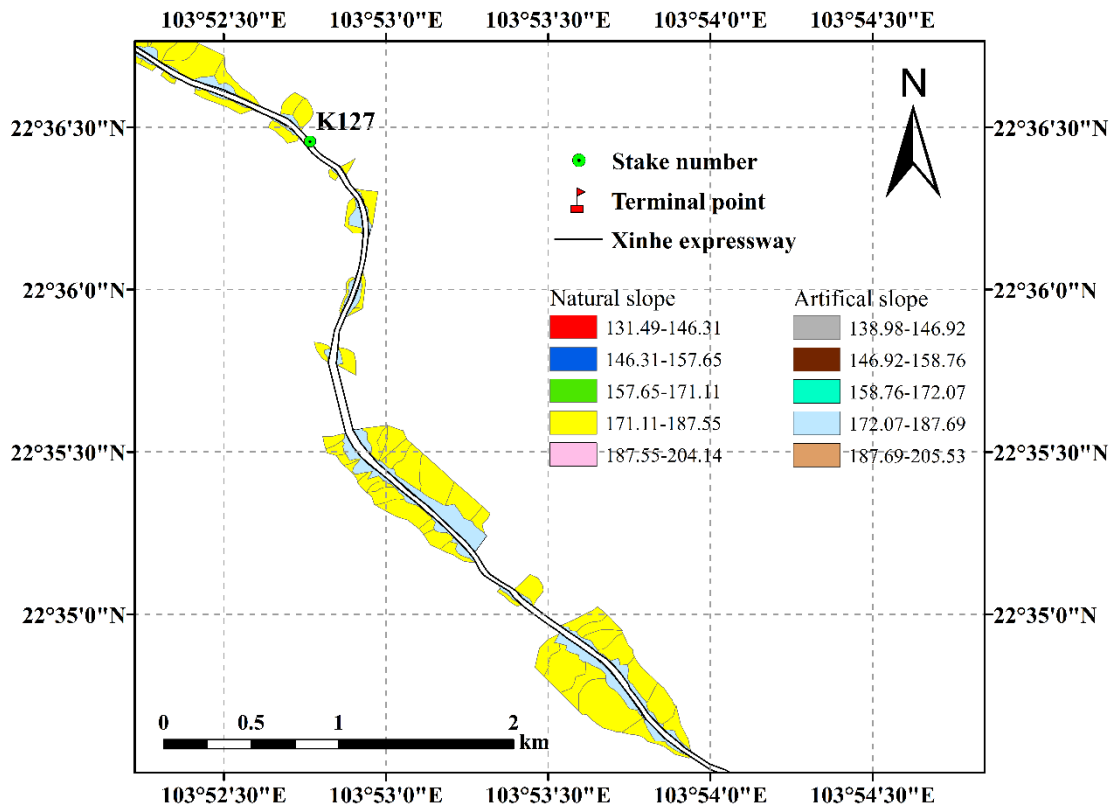
The secondary rainfall data of 16 rainfall instances along Xinhe Expressway were obtained by interpolation because the values for internal rainfall and the rainfall intensity of a single prediction unit are the same. Therefore, the R -value was calculated by using the average rainfall and rainfall intensity of the unit. Only the spatial distribution map of the rainfall erosivity factors in certain sections (June 5, 2014) is shown because of space constraints (Figures 5 and 6).



333

334

Figure 5. Spatial distribution map of rainfall erosivity factors (K127-K139+800)



335

336

Figure 6. Spatial distribution of rainfall erosion factor in typical a section of a highway

337 3.2.2 Soil erodibility factor (K)

338 The soil data of a slope in each section were obtained by sampling according to the spatial
339 distribution map of soil types in the study area and by dividing the linear distribution of the soil.
340 The K value was calculated by applying Formula 4 to obtain the soil erodibility factor values of
341 each slope (Sharply and Williams, 1990) (Tables 3 and 4; see supplementary material/appendices).

$$342 \quad K = 0.2 + 0.3e^{[0.0256SAN(1-SIL/100)]} \times \left(\frac{SIL}{CLA + SIL} \right)^{0.3} \times \left[1 - \frac{0.25C}{C + e^{3.72-2.95C}} \right] \times \left[1 - \frac{0.75N_1}{SN_1 + e^{22.9SN_1-5.51}} \right] \quad (4)$$

343 In the formula, SAN, SIL, CLA and C represent sand grains (0.05–2 mm), powder (0.002–
344 0.05 mm), clay (<0.002 mm) and organic carbon content (%), respectively; $SN_1=1-SAN/100$.

345

346 3.2.3 Calculation of topographic factors in natural slope catchments

347 (1) Slope length factor

348 On the basis of the topographic map (1:2000 scale) and highway design of Xinhe Expressway,
349 the slope length factor of the slope catchment was calculated by using DEM data with 0.5 m
350 spatial resolution generated by ArcGIS. The natural slope catchment was divided into less than 1°,
351 1°–3°, 3°–5° and greater than or equal to 5° by using the ‘reclassify’ tool in ArcGIS. The L factor
352 algorithm of Moore and Burch (1986) was utilised in the operation formulas (Formulas (5) and
353 (6)).

$$354 \quad L = \left(\frac{\lambda}{22.13} \right)^m \quad (5)$$

$$355 \quad \lambda = flowacc \cdot cellsize, \quad (6)$$

356 where L is normalised to the amount of soil erosion along the slope length of 22.13 m, λ is the
357 slope length, $flowacc$ is the total number of contributing pixels for each pixel that is higher than
358 the pixel and cell size refers to the DEM resolution (0.5m). m is a variable length-slope exponent.

359 Formula (7) is expressed as

$$360 \quad m = \begin{cases} 0.2 & \theta < 1^\circ \\ 0.3 & 1^\circ \leq \theta < 3^\circ \\ 0.4 & 3^\circ \leq \theta < 5^\circ \\ 0.5 & \theta \geq 5^\circ \end{cases} \quad (7)$$

361 where θ is the slope.

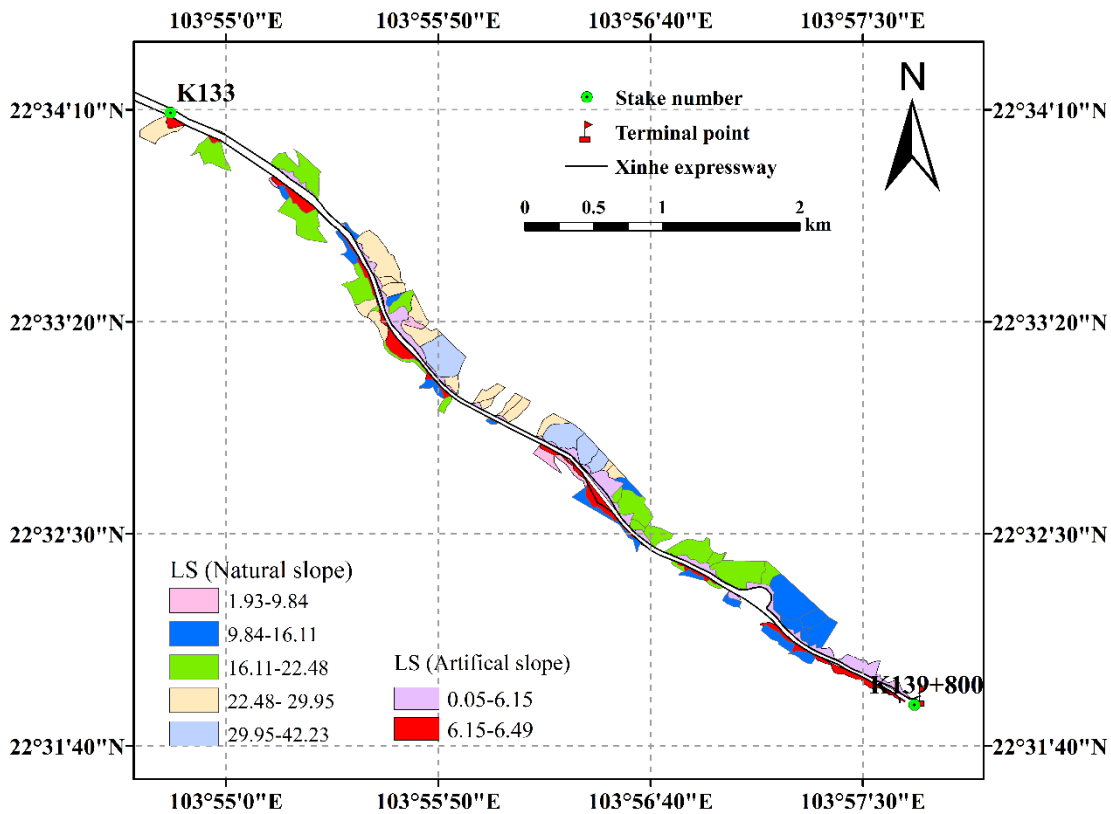
362 (2) Slope factor

363 The S factor was calculated as follows. If the slope was less than 18° , then the formula of
 364 McCool et al. (1987) was used. If the slope was greater than 18° , then the formula of Liu et al.
 365 (2000) was adopted. Formula (8) is expressed as

$$366 \quad S = \begin{cases} 10.8 \cdot \sin \theta + 0.03 & \theta < 9^\circ \\ 16.8 \cdot \sin \theta - 0.05 & 9^\circ \leq \theta < 18^\circ \\ 21.9 \cdot \sin \theta - 0.96 & \theta \geq 18^\circ \end{cases} \quad (8)$$

367 The DEM data were processed by ArcGIS to obtain slope data. The slope values of each
 368 prediction unit were extracted by using the Zonal statistics tool. With the classification tool in
 369 ArcGIS, the slope of the highway catchment of Xinhe was divided into less than 9° , $9-18^\circ$ and
 370 greater than or equal to 18° .

371 The S values of the slope catchments under the three slope grades were calculated by
 372 combining Formula (8) with ArcGIS techniques. The LS values of the slope prediction units are
 373 shown in Figure 7.



374

375

Figure 7. Spatial distribution map of topographic factors (K134–K139)

376 3.2.4 Calculation of topographic factors of artificial slopes

377 (1) Slope length factor

378 The method of Chen Zongwei (2010) was used for the calculation of the *LS* factor of the
379 artificial slopes, and the calculation method for the topographic factors of the artificial slopes of
380 Xinha Expressway was modified. The slope length factor (L_a) was calculated using Formulas (5)
381 and (6). The slope length index (m_a) was measured by conducting a runoff plot experiment and
382 calculated using Formula (9).

383
$$m_a = \log_{\frac{\lambda_1}{\lambda_2}} \frac{A_1}{A_2}, \quad (9)$$

384 where A_1 and A_2 are the soil erosion intensity values of two slopes when the slope lengths are λ_1
385 and λ_2 , respectively (i.e. the specifications of the two slopes are the same except for slope length).
386 The soil erosion amounts under 30 erosion rainfall conditions were monitored in the runoff field
387 of Xiao Xinzhai in Mengzi City in 2014–2015 (Table 5). The m_a value under each rainfall
388 condition was calculated using Formula (9) according to the monitoring value of soil erosion
389 amount. The average value of m_a was 0.32, and it was regarded as the m_a value of the artificial
390 slope length factor (Table 6).

391

392 (2) Slope factor

393 The calculation of the slope factor was based on the method of Chen Zongwei (Chen et al.,
394 2010). Six runoff plots were established in the Xiao Xinzhai runoff field of Mengzi City. Soil
395 erosion intensity under the slope conditions of 1:1.5, 1:1.0 and 9:100 was monitored. Then, the
396 slope factor for the slope condition was obtained using Formula (10).

397
$$S_\theta = \frac{A_\theta}{A}, \quad (10)$$

398 where S_θ represents the slope factor when the slope is θ , A_θ represents the soil erosion intensity
399 when the slope is θ (t/hm²) and A represents the soil erosion intensity when the slope is 9% (t/hm²).
400 The three slope conditions (1:1.5, 1:1.0 and control slope of 9:100) in the soil erosion monitoring
401 experiment were combined with Formula (10) to calculate the slope factor values of the two

402 slopes (1:1.5 and 1:1.0) under 30 rainfall conditions. The average factors of the slopes under the
 403 1:1.5 and 1:1.0 slope conditions were 7.28 and 14.49, respectively (Table 7).

404 After the slope design drawings were digitised by ArcGIS, the slope and length values of each
 405 artificial slope prediction unit were determined according to design specifications. The slope
 406 length value of each artificial slope prediction unit was regarded as the horizontal projection
 407 length of the cement frame. The slope length of the six arris brick revetments was 0. Formulas (5),
 408 (6), (9) and (10), in combination with the slope length factor and m_a and S_θ values, were used to
 409 calculate the value of LS of each artificial slope prediction unit.

410 **Table 7.** Calculation results of the slope factor

Time of the second rainfall	S_{46}	S_{56}
2014.06.05	7.23	14.52
2014.06.07	7.25	14.47
2014.06.17	7.25	14.41
2014.06.28	7.33	14.62
2014.07.01	7.28	14.57
2014.07.13	7.27	14.57
2014.07.20	7.28	14.52
2014.08.02	7.20	14.43
2014.08.12	7.23	14.46
2014.08.26	7.27	14.60
2014.08.29	7.24	14.44
2014.09.02	7.25	14.56
2014.09.04	7.33	14.72
2014.09.17	7.30	14.32
2014.09.20	7.28	14.49

2014.10.05	7.33	14.73
2015.07.04	7.23	14.36
2015.07.15	7.24	14.32
2015.07.24	7.17	14.15
2015.07.28	7.39	14.68
2015.08.13	7.28	14.47
2015.08.19	7.33	14.53
2015.08.26	7.35	14.47
2015.09.03	7.22	14.47
2015.09.12	7.28	14.47
2015.09.17	7.29	14.48
2015.09.25	7.28	14.47
2015.10.03	7.27	14.53
2015.10.08	7.36	14.71
2015.10.12	7.40	14.26
Average	7.28	14.49

411 *Note: S_{xy} represents the slope factor value simultaneously solved by erosion intensity values for monitoring plots*
412 *numbered x and y.*

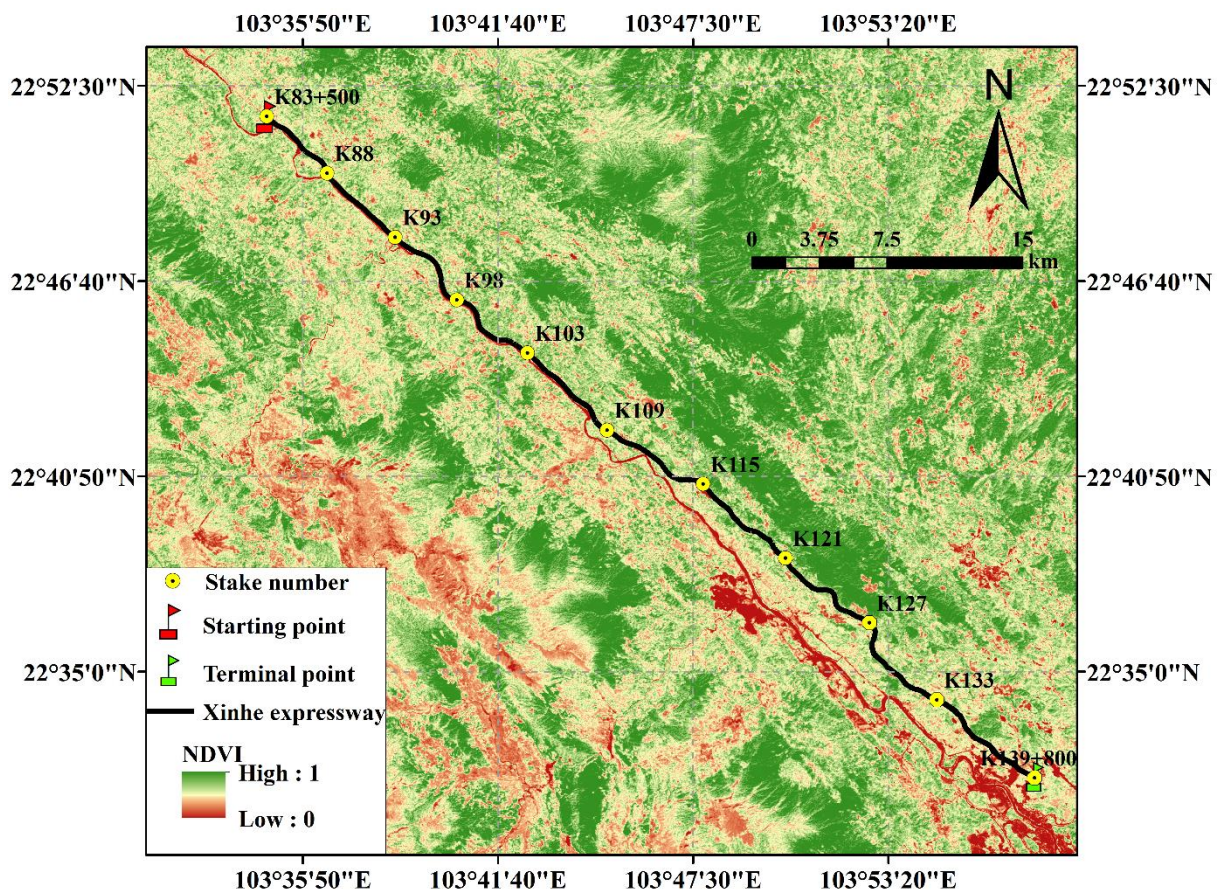
413

414 3.2.5 Cover and management practice factor

415 The *C* factor after topographic analysis is vital in soil loss risk control. In the RUSLE model,
416 the *C* factor is used to depict the effects of vegetation cover and management practices on the soil
417 erosion rate (Vander-Knijff et al., 2000; Prasannakumar et al., 2011; Alkharabsheh et al., 2013).
418 The *C* factor is defined as the loss ratio of soils from cropped land under specific conditions to the
419 corresponding loss from clean-tilled and continuous fallow (Wischmeier and Smith, 1978).
420 Datasets from satellite remote sensing were initially used to assess the *C* factor due to the various
421 land cover patterns with severe spatial and temporal variations mainly at the watershed scale
422 (Vander-Knijff et al., 2000; Li et al., 2010; Chen et al., 2011; Alexakis et al., 2013). By taking full

423 advantage of NDVI data, C was calculated according to the equation of Gutman and Ignatov
 424 (1998) (i.e. Formula (11)). Then, the vegetation coverage data were corrected by examining a
 425 sample plot every 2 km along the study area. The algorithm for calculating f was adopted from the
 426 work of Tan et al. (2005) (i.e. Formula (11)). Finally, accurate vegetation coverage data were
 427 obtained (Figure 8). The C factor map of the soil erosion prediction unit for the slope catchment
 428 area is shown in Figure 9.

429
$$C = 1 - \frac{NDVI - NDVI_{\min}}{NDVI_{\max} - NDVI_{\min}} \quad (11)$$



430
 431

Figure 8. Vegetation coverage along Xinhe Expressway

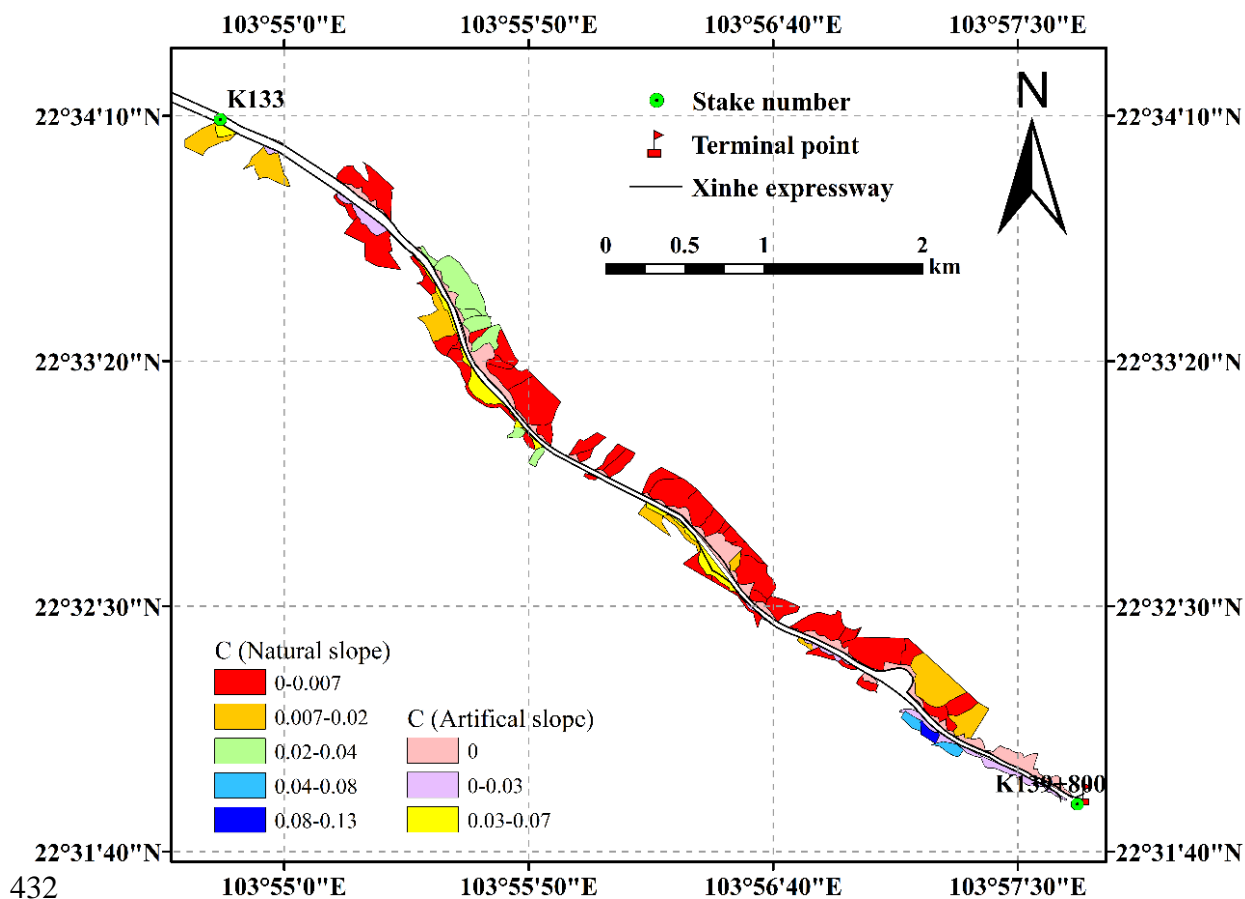


Figure 9. Spatial distribution map of the cover and management practice factor

3.2.6 Soil and water conservation measures

The land use types in the natural slope catchment area were classified as cultivated, forest, construction and difficult lands. Through a field investigation and visual judgment, the water conservation measures of farmland and forestland were identified as contour belt tillage, horizontal terrace and artificial slope catchment area, including cement frame and six arris brick revetments. The *P* values of the cement frame and the six arris brick revetments, which were determined by using the area ratio method, were 0.85 and 0.4, respectively. The *P* values of the soil and water conservation measures are shown in Table 8.

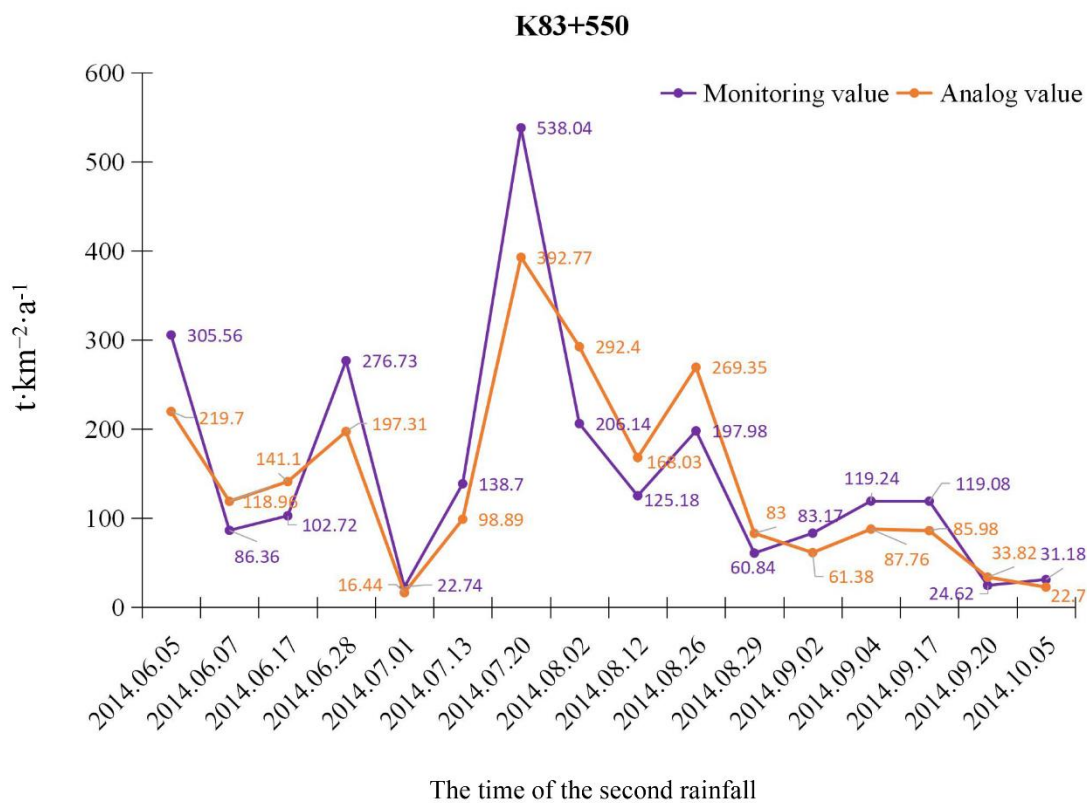
Table 8. *P* values of different slope types

Slope type	Cement frame	Hexagonal brick	Contour strip tillage	Level bench/terrace	Construction land	Difficult to use land	Others
<i>P</i>	0.85	0.4	0.55	0.03	0	0.2	1

444 **3.3 Validation of model simulation accuracy**

445 Soil erosion in three monitoring areas under 16 erosive rainfall conditions was monitored in
 446 2014. No rainfall occurred in the 24 h before each rainfall event, and the disturbance of antecedent
 447 rainfall on soil erosion on the slopes was excluded. After estimating the historical soil loss of each
 448 slope prediction unit, the results were compared with data from the three monitoring plots along
 449 the side slope of Xinhe Expressway (Figures 10–12).

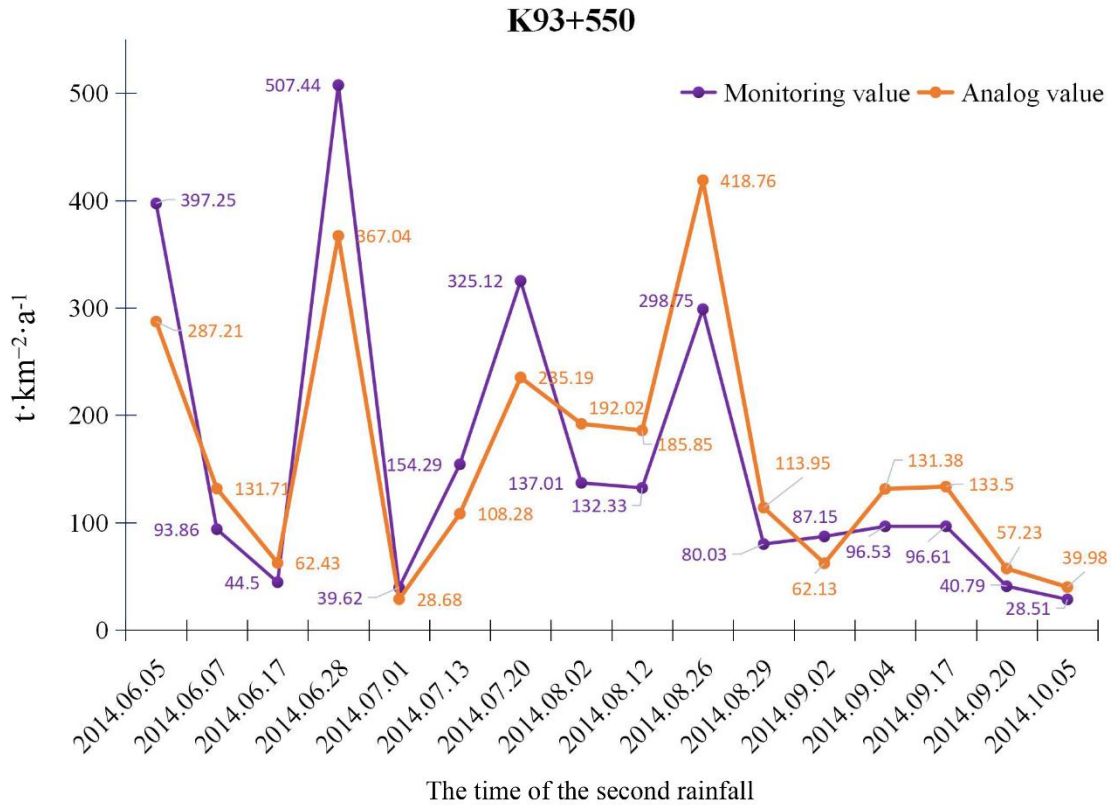
450



451

452

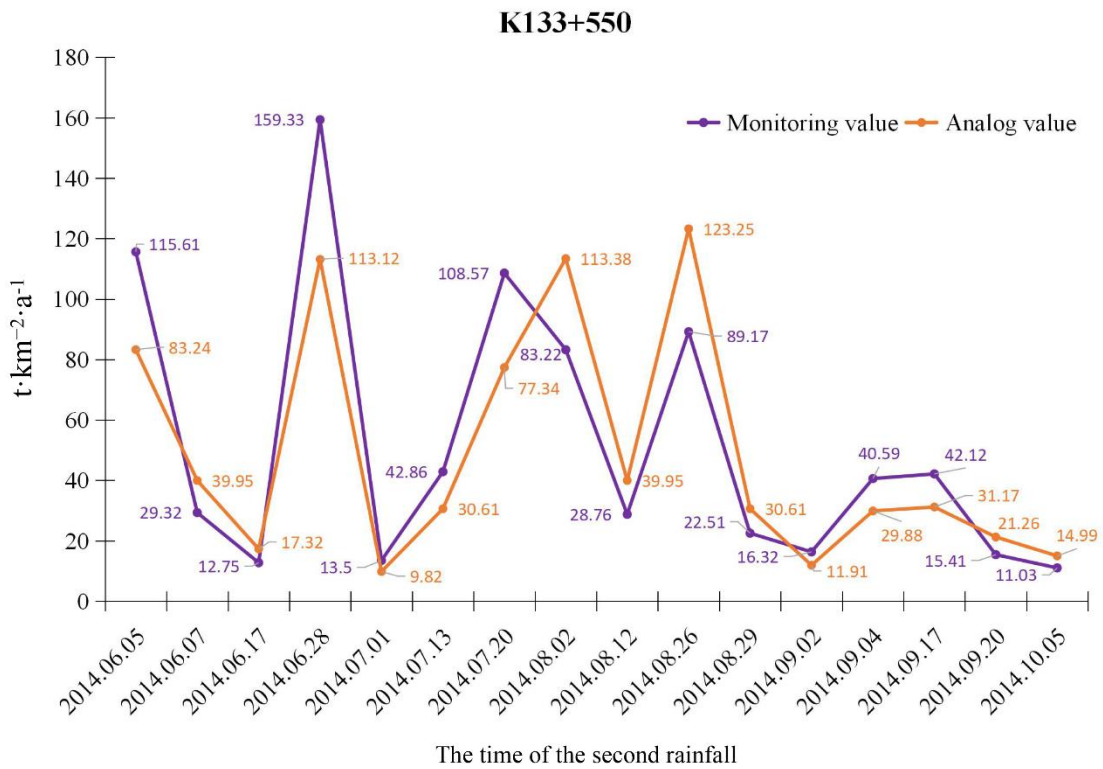
Figure 10. Comparison of model prediction and monitoring results (K83+550)



453

454

Figure 11. Comparison of model prediction and monitoring results (K93+550)



455

456

Figure 12. Comparison of model prediction and monitoring results (K133+550)

457

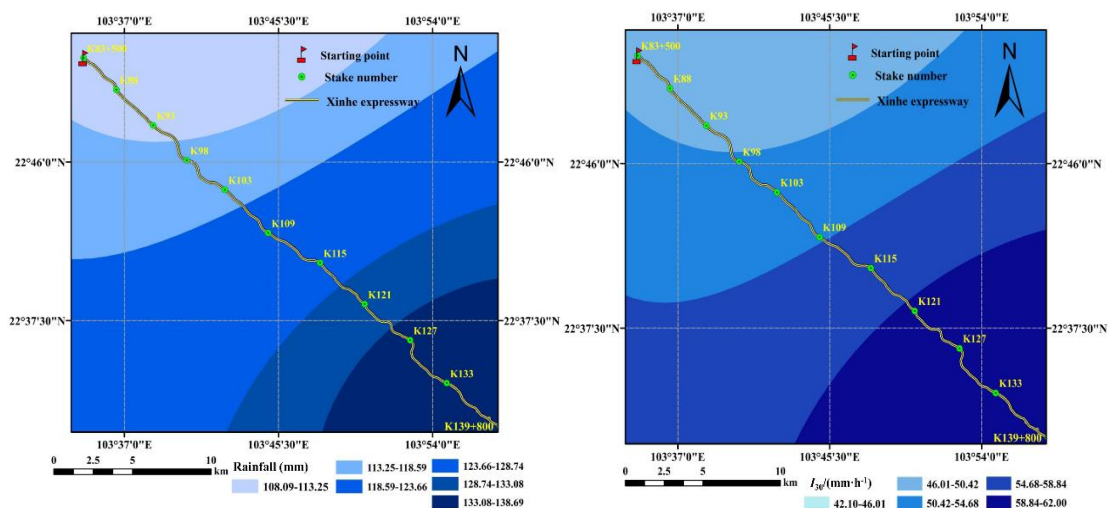
458 The error analysis showed that the absolute errors of the three monitoring areas under the 16
 459 rainfall conditions were 47.15, 52.52 and 16.27 $t \cdot km^{-2} \cdot a^{-1}$, and the overall average absolute error
 460 was 38.65 $t \cdot km^{-2} \cdot a^{-1}$. The average relative errors were 31.80%, 35.49% and 32.26%, and the
 461 overall mean relative error was 31.18%. The root mean square errors were 59.44, 65.6, and 20.95,
 462 all of which were within the acceptable range. The Nash efficiency coefficient of the model was
 463 0.67, which is between 0 and 1, thereby showing that the model's accuracy satisfied the
 464 requirements. The calculation results are shown in Tables 10–12 (see supplementary
 465 material/appendices).

466 The northern and flat terrains of the southern region had a small simulation error because of
 467 the high and low areas of the central region of the terrain, which resulted in a slightly lower
 468 accuracy than that for the southern region. The absolute error of the simulation was large under
 469 heavy rainfall conditions. On the one hand, this result may be caused by the artificial error in
 470 sediment collection in the area. On the other hand, the model itself may be defective.

471

472 3.4 Application of early warning of soil erosion to the mountain expressway

473 The rainfall data and I_{30} values in the 20 years covered by the study were obtained from the
 474 meteorological departments of Mengzi, Pingbian, Jinping and Hekou counties in Yunnan Province.
 475 Rainfall and its intensity were interpolated by co-kriging, which was introduced into the elevation
 476 and geographical position (Figures 13 and 14).



477

478 **Figure 13.** Rainfall interpolation results under 20-year return period

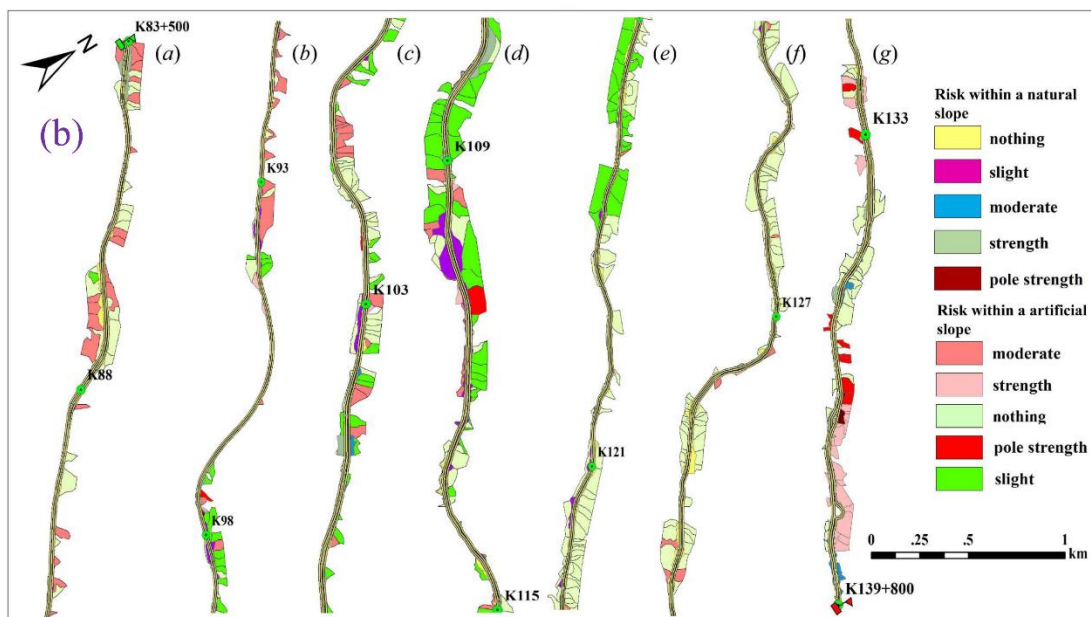
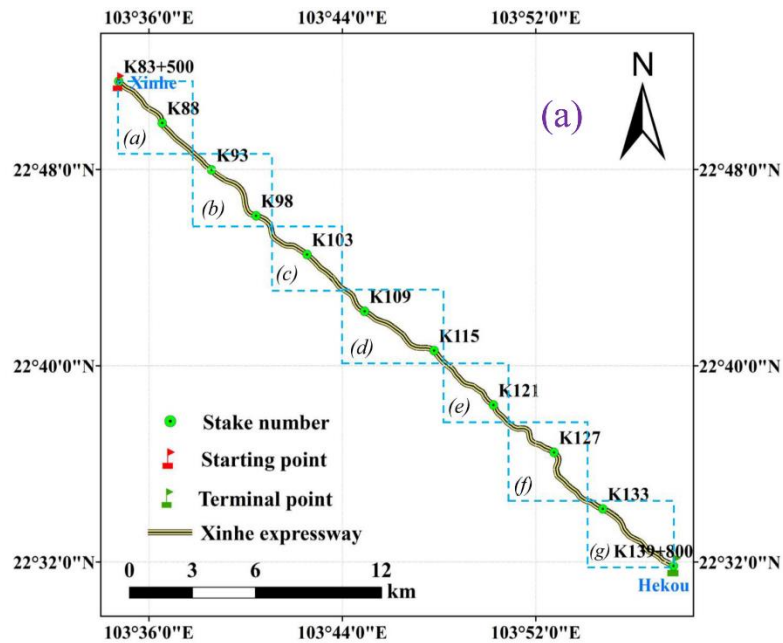
479

Figure 14. Rainfall intensity interpolation results under 20-year return period

480

The total soil erosion amount of each prediction unit for the 20-year **return period** rainfall
 481 data was obtained by simulation according to the classification standards of soil erosion intensity.

482 The prediction results were classified as ‘no risk’, ‘slight risk’, ‘moderate risk’, ‘high risk’ and
 483 ‘extremely high risk’ (Figure 15(a) (b)).



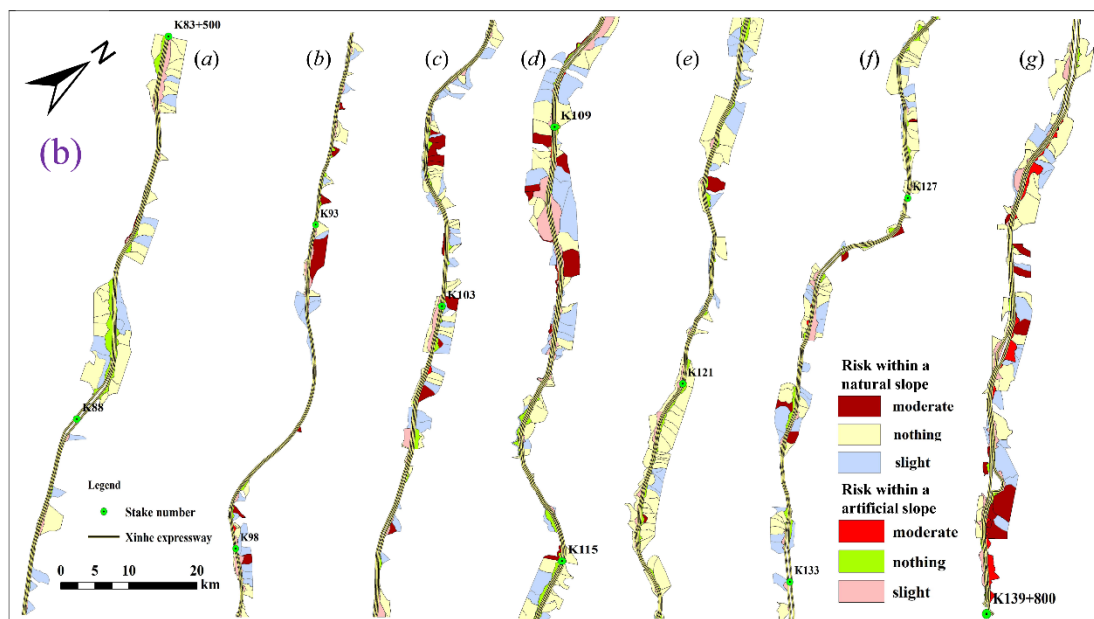
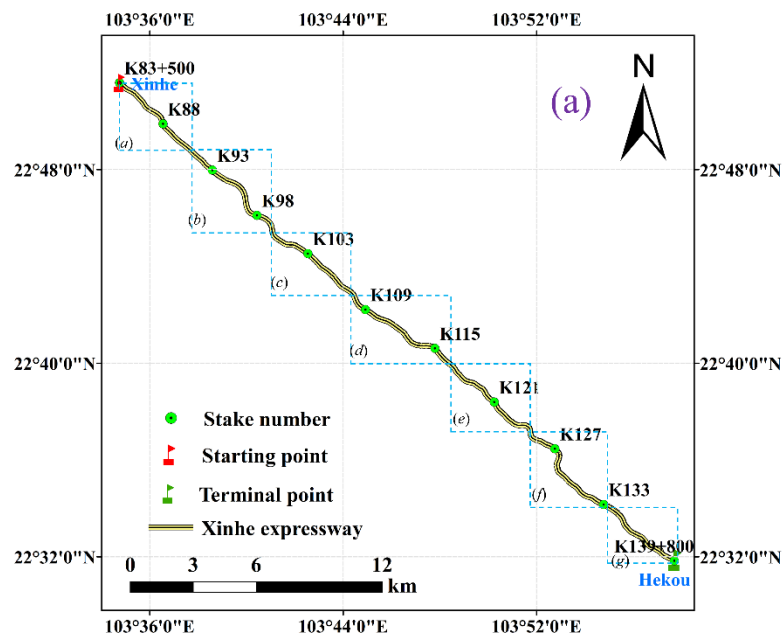
484
 485

Figure 15(a)(b). Risk analysis of soil loss under 20-year return period rainfall conditions

486 The grading results showed that the percentage of prediction units classified as having low
 487 and mild risks of soil loss was 88.60%. Given that the risk of soil erosion is low in these areas,
 488 road traffic safety is not affected. The percentage of prediction units classified as having a
 489 moderate risk was 4.29%. The risk of soil erosion in these areas is relatively low under general
 490 rainfall intensity conditions. However, with high rainfall intensity, a certain scale of soil erosion
 491 disaster could occur. The percentage of prediction units labelled as ‘high risk’ and ‘extremely high

492 risk' was 7.11%. The risk of soil erosion is high in these units. For example, from K134+500 to
 493 K135+500 (1000 m), the average soil erosion amount on both sides of the slope for the 20-year
 494 **return period** rainfall amount reached $1757 \text{ t} \cdot \text{km}^{-2} \cdot \text{a}^{-1}$. Even if only a portion of the sediment is
 495 deposited on the road, road safety will still be affected.

496 Similarly, the risk of soil erosion was analysed according to the grading standard of **soil loss**
 497 risk under the 20-year **return period** rainfall condition. This analysis was performed by simulating
 498 the soil erosion amount of each prediction unit for the 1-year **return period** rainfall amount (Figure
 499 16(a)(b)).



500
 501

Figure 16(a)(b). Risk analysis of soil and water loss for the 1-year return period rainfall amount

502 The results indicated that the risk percentages of the prediction units for no soil erosion and
503 mild soil erosion were 78.00% and 17.92%, respectively. Given that the risk of soil erosion is low
504 in these areas, the safety of road traffic is not affected. The risk percentage of prediction units for
505 mild soil erosion was 6.08%. Therefore, the layout of soil and water conservation measures in
506 these areas should be rationally adjusted. Moreover, comprehensive management of their slopes
507 should be strengthened, and plant and engineering measures should be applied comprehensively to
508 conserve soil and water in these regions. Inspections must be reinforced, and motorists should be
509 reminded to focus on traffic safety during rainy seasons. Most of the artificial slopes covered by
510 the study area are made of six arris brick revetment; that is, the amount of soil erosion is small,
511 and the frame-type cement slope protection against soil erosion is sturdier than those in other areas.
512 Slope protection measures should be rationally adjusted according to the predicted results. We
513 may adopt ecological slope protection technologies to slow down the roadbed slope and thus keep
514 the slope stable. For example, the spraying and planting technology for bolt hanging nets can be
515 used to build a layer of planting matrix that can grow and develop on the weathered rock slope
516 because it can resist the porous and stable structure of the scouring. Technologies for masonry
517 wall maintenance and honeycomb grid revetment protection can also be used. Various other
518 technologies can be adopted to prevent and control soil erosion, and they can beautify the
519 landscape environment of the road area whilst ensuring road traffic safety.

520

521 **4 Discussion**

522 Slope is the main factor of the **soil loss** caused by highways. Thus, slope is crucial for
523 prediction and early warning systems. A highway slope can be divided into natural and
524 engineering (artificial) slopes, and the RUSLE model can be used to predict soil erosion on natural
525 slopes. Disregarding rainfall erosivity variations, we found that the methods of model parameter
526 acquisition for literature analysis and for comparison of areas of the same type are consistent
527 (Yang 1999; Yang 2002; Peng et al., 2007; Zhao et al., 2007; Chen et al., 2014; Zhu et al., 2016).
528 After comparing the monitoring data with runoff plots, we discovered that the error between the
529 predicted value and the monitoring value calculated by the RUSLE model is negligible (Yang
530 1999; Yang 2002; Li et al., 2004). These findings indicate that the prediction results of the model
531 are reliable. In the prediction of erosion on engineering (artificial) slopes, previous studies
532 emphasised surface disturbance during construction (He, 2004; Liu et al., 2011; He, 2008; Hu,
533 2016; Zhang et al., 2016; Song et al., 2007) but did not consider soil erosion as a result of the
534 construction. In the process of predicting **soil loss** in engineering slopes by using the RUSLE
535 model, the correction of the conservation support factor (i.e. cement block and hexagonal brick) is
536 often ignored (Zhang, 2011; Morschel et al., 2004; Correa and Cruz, 2010). In addition, most

537 cases use RUSLE modelling to predict the soil erosion on highway slopes. Remote sensing is
538 usually based on grid data and does not consider catchment units (Islam et al., 2018; Villarreal et
539 al., 2016; Wu and Yan 2014; Chen et al., 2010).

540 In this study, we analysed the characteristics of soil erosion during expressway construction
541 to improve several aspects of previous research. First, we divided the highway slope into natural
542 and artificial units and calculated the amount of soil loss from the slope surface to the pavement
543 based on the slope surface catchment unit. Given that this approach is more in line with the actual
544 situation than previous methods, the findings of the present study can be popularised. Second, we
545 considered the spatial heterogeneity of the linear engineering of an expressway. The rainfall factor
546 was spatially interpolated to compensate for the limitations on rainfall data, which were usually
547 used by previous studies. Third, we modified the parameters of the artificial slope through an
548 actual survey, runoff plot observation and other methods, and the parameters of the artificial slope
549 were corrected by referring to the form of the project and the utilised materials.

550

551 **5 Conclusions**

552 In this study, we used the revised universal soil loss equation as the prediction model for soil
553 loss on slopes, predicting the soil loss on highway slopes and simulating the risk of soil loss along
554 the mountain expressway. We not only scientifically predict the amount of soil erosion caused by
555 highway construction in mountain areas but also provide a scientific basis for the prevention and
556 control of soil erosion and rational allocation of prevention and control measures. The error
557 analysis of the actual observation data showed that the overall average absolute error of each
558 monitoring area was $38.65 \text{ t}\cdot\text{km}^{-2}\cdot\text{a}^{-1}$, the average relative error was 31.18%, the root mean square
559 error was between 20.95 and 65.64 and the Nash efficiency coefficient was 0.67. The method of
560 soil loss prediction adopted in this work generally has a smaller error and higher prediction
561 accuracy than other models, and it can satisfy prediction requirements. The risk grades of soil loss
562 along the slope of Xinhe Expressway were divided into 20- and 1-year return period rainfall
563 conditions based on simulated predictions. The results showed that the percentage of slope areas
564 with high and extremely high risks was 7.11%. These areas are mainly located in the K109+500–
565 K110+500 and K133–K139+800 sections. Therefore, relevant departments should strengthen
566 disaster prevention and reduction efforts and corresponding water and soil conservation initiatives
567 in these areas.

568

569 **6 Acknowledgment**

570 This study was jointly supported by the Yunnan Provincial Communications Department Project
571 (2012-272-(1)) and the Yunnan Provincial Science and Technology Commission Project
572 (2014RA074).

573

574 **7 References**

575 Alexakis, D., Diofantos, G., Hadjimitsis, A.: Integrated use of remote sensing, GIS and
576 precipitation data for the assessment of soil erosion rate in the catchment area of “Yialias” in
577 Cyprus. *Atmospheric Research*, 131, 108-124, 2013.

578 Alkharabsheh, M.M., Alexandridis, T.K., Bilasb, G., Misopolinos, N.: Impact of land cover change
579 on soil erosion hazard in northern Jordan using remote sensing and GIS. Four decades of
580 progress in monitoring and modeling of processes in the soil-plant-atmosphere system:
581 applications and challenges. *Procedia Environmental Science*, 19, 912-921, 2013.

582 Angulomartínez, M., and Beguería, S.: Estimating rainfall erosivity from daily precipitation
583 records: a comparison among methods using data from the ebro basin (NE Spain). *Journal of*
584 *Hydrology*, 379(1): 111-121, 2009.

585 Bakr, N., Weindorf, D. C., Zhu, Y. D., Arceneaux, A. E., Selim, H. M.: Evaluation of
586 compost/mulch as highway embankment erosion control in Louisiana at the plot scale. *Journal*
587 *of Hydrology*, 468-469(6): 257-267, 2012.

588 Bosco, C., De Rigo, D., Dewitte, O., Poesen, J., and Panagos, P.: Modelling soil erosion at
589 European scale: towards harmonization and reproducibility. *Natural Hazards & Earth System*
590 *Sciences*, 2(4), 2639-2680, 2015.

591 Cai, C. F., Ding, S. W., Shi, Z. H., Huang, L., Zhang, G. Y.: Study of Applying USLE and
592 Geographical Information System IDRISI to Predict Soil Erosion in Small Watershed.
593 *Journal of Soil and Water Conservation*. 14(2): 19-24, 2000.

594 Chen, B. H.: The study on multivariate spatial interpolation method of precipitation in
595 mountainous areas. Beijing Forestry University, 2016 (in Chinese).

596 Chen, F., Zeng, M. G., and Zhou, Z. H.: Evaluation for Ecological Benefits of Greening on
597 Expressways in Mountainous Area. *Technology of Highway and Transport*, 1:139-143, 2015
598 (in Chinese).

599 Chen, S. X., Yang, X. H., Xiao, L. L., Cai, Y. H.: Study of Soil Erosion in the Southern Hillside
600 Area of China Based on RUSLE Model. *Resources Science*, 36(6): 1288-1297, 2014 (in
601 Chinese).

602 Chen, T., Niu, R. Q., Li, P. X., Zhang, L. P., Du, B.: Regional soil erosion risk mapping using
603 RUSLE, GIS, and remote sensing: a case study in Miyun watershed, North China.
604 *Environmental Earth Sciences*, 63(3), 533-541, 2011.

605 Chen, Y. J., Sun, K. M., and Zhao, Y.: Experiment on the effect of rule caused by slope angle on
606 sand and runoff under the condition of ecological protected slope. *Journal of Water Resources*
607 *& Water Engineering*, 21(4):55-59, 2010 (in Chinese).

608 Chen, Z. W., He, F., and Wang, J. J.: Revises of Terrain Factors of Roadbed Side Slope in
609 Universal Soil Loss Equation. *HIGHWAY*, 12:180-185, 2010 (in Chinese).

- 610 Chen, Z. W., He, F., and Wang, J. J.: Revises of Terrain Factors of Roadbed Side Slope in
611 Universal Soil Loss Equation. *HIGHWAY*, 12:180-185, 2010 (in Chinese)
- 612 Chen, Z. W., He, F., Wang, J. J.: Revises of Terrain Factor of Roadbed Side Slope in Universal
613 Soil Loss Equation. *HIGHWAY*, (12):180-185, 2010 (in Chinese).
- 614 Correa, C. M. C., Cruz, J.: Real and estimative erosion through RUSLE from forest roads in
615 undulated at heavily undulated relief. *Revista Árvore*, 34(4): 587-595, 2010.
- 616 Cunha, E. R. D., Bacani, V. M., Panachuki, E.: Modeling soil erosion using RUSLE and GIS in a
617 watershed occupied by rural settlement in the Brazilian Cerrado. *Natural Hazards*, 85, 1-18,
618 2017.
- 619 Dong, H., Zeng, H.: Discussion on the current situation and the future of China highway
620 construction. *Technology & Economy in Areas of Communication (TEAC)*, 5(3):17-18, 2003
621 (in Chinese).
- 622 Fei, X. H., Song, Q. H., Zhang, Y. P., Liu, Y. T., Sha, L. Q., Yu, G. R., Zhang, L. M., Duan, C. Q.,
623 Deng, Y., Wu, C. S., Lu, Z. Y., Luo, K., Chen, A. G., Xu, K., Liu, W. W., Huang, H., Jin, Y. Q.,
624 Zhou, R. W., Grace, J.: Carbon exchanges and their responses to temperature and
625 precipitation in forest ecosystems in Yunnan, Southwest China. *Science of The Total
626 Environment*, 616: 824-840, 2017.
- 627 Feng, Q., and Zhao, W. W.: The study on cover-management factor in USLE and RUSLE: a
628 review. *ACTA ECOLOGICA SINICA*, 34(16):4461-4472, 2014 (in Chinese).
- 629 Fenta, A. A., Yasuda, H., Shimizu, K., Haregeweyn, N., and Negussie, A.: Dynamics of Soil
630 Erosion as Influenced by Watershed Management Practices: A Case Study of the Agula
631 Watershed in the Semi-Arid Highlands of Northern Ethiopia. *Environmental Management*,
632 58(5): 1-17, 2016.
- 633 Foster, G. R., Weesies, G. A., McCool, D. K., Joder, D. C., Renard, K. G.: Revised Universal Soil
634 Loss Equation User's Manual. Gov. Print. Office, Washington D.C. (48p), 1999.
- 635 Gong, J., and Yang, P.: Study on the Layout of Soil and Water Conservation Monitoring Sites
636 during the Construction of Mountain Highways-Case Study of Enlai, Enqian Highway.
637 *Subtropical Soil and Water Conservation*, 28(1):9-11, 2016 (in Chinese).
- 638 He, F.: Prediction of soil erosion in foundation slope of South Hubei Road Based on RUSLE.
639 Beijing Normal University, 2008 (in Chinese).
- 640 He, X. W.: Study on prediction of soil erosion in Road area. Beijing Normal University, 2004 (in
641 Chinese).
- 642 Hu, L.: Study on development and mechanism of water Erosion and Ecological water erosion
643 control technology of Highway slope in Cold Region. Xi'an University of technology, 2016
644 (in Chinese).
- 645 Islam, M. R., Wan, Z. W. J., Lai, S. H., Osman, N., Din, M. A. M., Zuki, F. M.: Soil erosion
646 assessment on hillslope of GCE using RUSLE model. *Journal of Earth System Science*,
647 127(4): 50, 2018.
- 648 Jia, Y. H., Dai, D. C., Liu, Y.: Performance Analyse and Evaluation of Freeway in China.
649 *JOURNAL OF BEIJING JIAOTONG UNIVERSITY*, 29(6):1-5, 2005 (in Chinese)

- 650 Jia, Z. R., Guo, and Z. Y.: Quantifying Evaluation Approach to Highway Soil Bioengineering.
651 Research of Soil and Water Conservation, 15(2):260-262, 2008 (in Chinese).
- 652 Jiang, M., Pan, X. Y., Nie, W. T.: Preliminary analysis of prevention and control of soil and water
653 loss in expressway project construction. Yangtze River, 48(12):61-64, 2017 (in Chinese).
- 654 Kateb, H. E., Zhang, H. F., Zhang, P. C., Mosandl, R. Soil erosion and surface runoff on different
655 vegetation covers and slope gradients: A field experiment in Southern Shaanxi Province,
656 China. Catena, 105(5): 1-10, 2013.
- 657 Kateb, H. E., Zhang, H. F., Zhang, P. C., Mosandl, R. Soil erosion and surface runoff on different
658 vegetation covers and slope gradients: A field experiment in Southern Shaanxi Province,
659 China. Catena, 105(5): 1-10, 2013.
- 660 Kinnell, P. I. A.: Applying the RUSLE and the USLE-M on hillslopes where runoff production
661 during an erosion event is spatially variable. Journal of Hydrology, 519:3328-3337, 2014.
- 662 Li, H., Chen, X. L., Kyoung, J. L., Cai, X. B., Myung S.: Assessment of soil erosion and sediment
663 Li, J. G., Dao, H. Y., Zhang, L., Zhang, H. K.: Soil and Water Loss Monitoring in the Dianchi
664 Watershed. Research of Soil and Water Conservation, 11(2): 75-77, 2004 (in Chinese).
- 665 Li, Y., Qi S., Cheng, B. H., Ma, J. M., Ma, C., Qiu, Y. D., Chen, Q. Y.: A Study on Factors of
666 Space-time Distributions of Precipitation in Ailao Mountain Area and Comparison of
667 Interpolation Methods. EARTH AND ENVIRONMENT, 45(6): 600-610 (in Chinese)
- 668 Lin, H. L., Zheng, S. T., and Wang, X. L.: Soil erosion assessment based on the RUSLE model in
669 the Three-Rivers Headwaters area, Qinghai-Tibetan Plateau, China. ACTA
670 PRATACULTURAE SINICA, 26(7):11-22, 2017 (in Chinese)
- 671 Liu, B. Y., Nearing, M. A., Shi, P. J., and Jia, Z. W.: Slope length effects on soil loss for steep
672 slopes. Soil Science Society of America Journal 64(5): 1759-1763, 2000.
- 673 Liu, J. T., Zhang, J. B.: Interpolation analysis of the spatial distribution of precipitation in
674 mountain area. Journal of Irrigation & Drainage, 25:34-38, 2006 (in Chinese)
- 675 Liu, S. L., Zhang, Z. L., Zhao, Q. H., Deng, L., Dong, S. K.: Effects of Road on Landscape Pattern
676 and Soil Erosion: A Case Study of Fengqing County, Southwest China. Chinese Journal of
677 Soil Science, 42(1): 169-173, 2011 (in Chinese).
- 678 Liu, W. Y.: Preliminary Study on R Index of Zhaotong Basin. Yunnan Forestry Science and
679 Technology, (2):24-26, 1999 (in Chinese)
- 680 Liu, X. Y.: Study on the slope stability and its rheological influence in Mountain highway. Central
681 South University, 2013 (in Chinese).
- 682 Liu, Z. Y., Zhang, X., Fang, R. H. Analysis of spatial interpolation methods to precipitation in
683 Yulin based on DEM. Journal of Northwest A&F University (Nat. Sci. Ed.), 38:227-234,
684 2010 (in Chinese)
- 685 Mccool, D. K., Brown, L. C., Foster, G. R., Mutchler, C. K., and Meyer, L. D.: Revised slope
686 steepness factor for the universal soil loss equation. Transactions of the ASAE-American
687 Society of Agricultural Engineers (USA), 30(5): 1387-1396, 1987.
- 688 Millward, A. A., and Mersey, J. E.: Adapting the rusle to model soil erosion potential in a
689 mountainous tropical watershed. Catena 38(2):109-129, 1999.

- 690 Molla, T., and Sisheber, B.: Estimating soil erosion risk and evaluating erosion control measures
691 for soil conservation planning at Koga watershed in the highlands of Ethiopia. *Solid Earth*, 8,
692 1-23, 2017
- 693 Moore, I. D., and Burch, G. J.: Physical basis of the length-slope factor in the universal soil loss
694 equation. *Soil Science Society of America Journal*, 50(5): 1294-1298, 1986.
- 695 Mori, A., Subramanian, S. S., Ishikawa, T., Komatsu, M. A Case Study of a Cut Slope Failure
696 Influenced by Snowmelt and Rainfall. *Procedia Engineering*, 189: 533-538, 2017.
- 697 Mori, A., Subramanian, S. S., Ishikawa, T., Komatsu, M. A Case Study of a Cut Slope Failure
698 Influenced by Snowmelt and Rainfall. *Procedia Engineering*, 189: 533-538, 2017.
- 699 Morschel, J., Fox, D. M., & Bruno, J. F.: Limiting sediment deposition on roadways: topographic
700 controls on vulnerable roads and cost analysis of planting grass buffer strips. *Environmental
701 Science & Policy*, 7(1): 39-45, 2004.
- 702 Mountain Region of Yunnan Province. *SCIENTIA GEOGRAPHICA SINICA*, 19(3):265-270,
703 1999 (in Chinese)
- 704 Panagos, P., Ballabio, C., Borrelli, P., Meusburger, K., Klik, A., Rouseva, S., Tadić, M.P.,
705 Michaelides, S., Hrabalíková, M., Olsen, P., Aalto, J., Lakatos, M., Rymaszewicz, A.,
706 Dumitrescu, A., Beguería, S., Alewell, C.: Rainfall erosivity in Europe. *Science of the Total
707 Environment*, 511:801-814, 2015.
- 708 Panagos, P., Borrelli, P., Meusburger, K., Yu, B., Klik, A., Lim, K.J., Yang, J.E., Ni, J., Miao, C.,
709 Chattopadhyay, N., Sadeghi, S.H., Hazbavi, Z., Zabihi, M., Larionov, G.A., Krasnov, S.F.,
710 Gorobets, A.V., Levi, Y., Erpul, G., Birkel, C., Hoyos, N., Naipal, V., Oliveira, P.T.S., Bonilla,
711 C.A., Meddi, M., Nel, W., Al Dashti, H., Boni, M., Diodato, N., Van Oost, K., Nearing, M.,
712 Ballabio, C. Global rainfall erosivity assessment based on high-temporal resolution rainfall
713 records. *Scientific Reports*, 7(1): 4175, 2017.
- 714 Panagos, P., Standardi, G., Borrelli, P., Lugato, E., Montanarella, L., Bosello, F.: Cost of
715 agricultural productivity loss due to soil erosion in the European union: from direct cost
716 evaluation approaches to the use of macroeconomic models. *Land Degradation &
717 Development*. 2018.
- 718 Panos, P., Cristiano, B., Pasquale, B., Katrin, M., Andreas, K., Svetla, R., Melita, P. T., Silas, M.,
719 Michaela, H., Preben, O., Juha, A., Mónica, L., Anna, R., Alexandru, D., Santiago, B., and
720 Christine, A.: Rainfall erosivity in Europe. *Science of the Total Environment*, 511: 801, 2015.
- 721 Peng, J., Li, D. D., Zhang, Y. Q.: Analysis of Spatial Characteristics of Soil Erosion in Mountain
722 Areas of Northwestern Yunnan Based on GIS and RUSLE. *Journal of mountain science*,
723 25(5): 548-556, 2007 (in Chinese).
- 724 Prasannakumar, R., Shiny, N., Geetha, H., Vijith, H.: Spatial prediction of soil erosion risk by
725 remote sensing, GIS and RUSLE approach: a case study of Siruvani river watershed in
726 Attapady valley, Kerala, India. *Environmental Earth Science*, 965-972, 2011.
- 727 Renard, K. G., Foster, G. R., Weesies, G. A., Mccool, D. K, and Yoder, D. C.: Predicting soil
728 erosion by water: a guide to conservation planning with the revised universal soil loss
729 equation (RUSLE). *Agriculture Handbook*, 1997.

- 730 Renard, K. G., Foster, G. R., Weesies, G. A., McCool, D. K., Yoder, D. C.: Predicting soil erosion
731 by water-a guide to conservation planning with the Revised Universal Soil Loss Equation
732 (RUSLE). United States Department of Agriculture, Agricultural Research Service (USDA-
733 ARS) Handbook No.703. United States Government Printing Office: Washington, DC. 1997.
- 734 Rick, D., Van, R., Matthew, E. H., and Robert J. H.: Estimating the LS Factor for RUSLE through
735 Iterative Slope Length Processing of Digital Elevation Data within ArclInfo Grid. *Cartography*,
736 30(1): 27-35, 2001.
- 737 Shamshad, A., Azhari, M. N., Isa, M. H., Hussin, W. M. A. W., and Parida, B. P.: Development of
738 an appropriate procedure for estimation of RUSLE EI₃₀ index and preparation of erosivity
739 maps for Pulau Penang in Peninsular Malaysia. *Catena*, 72(3): 423-432, 2008.
- 740 Sharpley, A. N., and Williams, J. R.: EPIC-erosion/productivity impact calculator: 2. User manual.
741 Technical Bulletin-United States Department of Agriculture, 4(4): 206-207, 1990.
- 742 Shi, Z. H., Cai, C. F., Ding, S. W., Wang, T. W., and Chow, T. L.: Soil conservation planning at the
743 small watershed level using RUSLE with GIS: a case study in the three gorge area of china.
744 *Catena*, 55(1): 33-48, 2004.
- 745 Shu, Z. Y., Wang, J. Y., Gong, W., Lv, X. N., Yan, S. Y., Cai, Y., Zhao, C. P.: Effects of compound
746 management in citrus orchard on soil micro-aggregate fractal features and soil physical and
747 chemical properties. *Journal of Nanjing Forestry University (Natural Sciences Edition)*, 41(5):
748 92-98, 2017.
- 749 Silburn, D. M.: Hillslope runoff and erosion on duplex soils in grazing lands in semi-arid central
750 Queensland. III. USLE erodibility (K factors) and cover-soil loss relationships. *Soil Research*,
751 49(49): 127-134, 2011.
- 752 Soil and Water Conservation Society. RUSLE user's guide. Soil and Water Cons. Soc. Ankeny, IA.
753 164pp, 1993.
- 754 Song, F. L., Ma, Y. H., Zhang, C. X., Yu, H. M., Hu, H. X., He, J. L., Huang, J. Y.: Research
755 progress on greening substrate material of ecological protection of expressway-side slope.
756 *Science of Soil and Water Conservation*, 6:57-61, 2008 (in Chinese).
- 757 Song, X. Q., Zhang, C. Y., Liu, J.: Formation of Soil and Water Loss and Its Characteristics in
758 Development and Construction Projects. *Bulletin of Soil and Water Conservation*, 27(5): 108-
759 113, 2007 (in Chinese).
- 760 Stanchi, S., Freppaz, M., Ceaglio, E., Maggioni, M., Meusburger, K., & Alewell, C., and Zanini,
761 E.: Soil erosion in an avalanche release site (Valle d'Aosta: Italy): towards a winter factor for
762 RUSLE in the Alps. *Natural Hazards & Earth System Sciences*, 14(7), 255-440, 2014.
- 763 Tan, B. X., Li, Z. Y., Wang, Y. H., Yu, P. T., Liu, L. B.: Estimation of Vegetation Coverage and
764 Analysis of Soil Erosion Using Remote Sensing Data for Guishuihe Drainage Basin. *Remote
765 sensing technology and application*. 20 (2): 215-220, 2005.
- 766 Tan, S. H., and Wang, Y. M.: Research Progress and Thinking of Bioengineering Techniques for
767 Slope Protection in Expressway. *Research of Soil and Water Conservation*, 11(3):81-84, 2004
768 (in Chinese).
- 769 Taye, G., Vanmaercke, M., Poesen, J., Wesemael, B. V., Tesfaye, S., Tekla, D., et al.: Determining
770 RUSLE P-and C-factors for stone bunds and trenches in rangeland and cropland, North
771 Ethiopia. *Land Degradation & Development*, 29(5), 2017.

- 772 Toy, T. J., Foster, G. R., Renard, K. G.: Soil Erosion: Processes, Prediction, Measurement, and
773 Control. 2002
- 774 Tresch, S., Meusburger, K., and Alewell, C.: Influence of slope steepness on soil erosion
775 modelling with RUSLE, measured with rainfall simulations on subalpine slopes. Bulletin of
776 Hokkaido Prefectural Agricultural Experiment Stations, 1995.
- 777 Vander-Knijff, J.M., Jones, R.J.A., Montanarella, L.: Soil Erosion Risk Assessment in Europe
778 EUR 19044 EN. Office for Official Publications of the European Communities, Luxembourg.
779 34, 2000.
- 780 Villarreal, M. L., Webb, R. H., Norman, L. M., Psillas, J. L., Rosenberg, A. S., Carmichael, S.:
781 Modeling landscape-scale erosion potential related to vehicle disturbances along the USA-
782 Mexico border. *Land Degradation & Development*, 27(4): 1106-1121, 2016.
- 783 Wang, C. J.: Regional Impaction and Evolution of Express Way Networks in China. *PROGRESS*
784 *IN GEOGRAPHY*, 25(6):126-137, 2006 (in Chinese)
- 785 Wang, H. J., Yang, Y., and Wang, W. J.: Prediction of Soil Loss Quantity on Side Slope of Freeway
786 Construction: Amendments to Main Parameters of USLE. *Journal of Wuhan University of*
787 *Technology (Transportation Science & Engineering)*, 29(1):12-15, 2005 (in Chinese).
- 788 Wang, K., and Gao, Z. L.: Analysis of Bioengineering Technology for Slope Protection of
789 Expressway: Taking Expressway from Ankang to the Border of Shaanxi and Hubei as an
790 Example. *Ecological Economy*, 31(5):155-159, 2015 (in Chinese).
- 791 Wang, L. H., Ma, B., and Wu, F. Q.: Effects of wheat stubble on runoff, infiltration, and erosion of
792 farmland on the Loess Plateau, China, subjected to simulated rainfall. *Solid Earth*, 8(2), 1-28,
793 2017.
- 794 Wang, W. Z., and Jiao, J. Y.: Quantitative Evaluation on Factors Influencing Soil Erosion in China.
795 *Bulletin of Soil and Water Conservation*, (st):1-20, 1996 (in Chinese).
- 796 Wang, W. Z., and Zhang, X. K.: Distribution of Rainfall Erosivity *R* Value in China. *Journal of soil*
797 *erosion and soil conservation*, 2(1): 7-18, 1995.
- 798 Wang, W. Z., Jiao, J. Y., Hao, X. P., Zhang, X. K., Lu, X. Q., Chen, F. Y., Wu, S. Y.: Study on
799 Rainfall Erosivity in China. *Journal of Soil and Water Conservation*, (4):7-18, 1995 (in
800 Chinese)
- 801 Wischmeier, W.H., Smith, D.D.: Predicting rainfall erosion losses: a guide to conservation
802 planning. In: USDA, Agriculture Handbook No. 537, Washington, DC, 1978.
- 803 Wischmerie, W. H., and Smith, D. D.: Predicting rainfall-erosion losses from cropland east of the
804 rocky mountains: a guide to conservation planning, 1965.
- 805 Wu, Y. L., Yan, L. J.: Impact of road on soil erosion risk pattern based on RUSLE and GIS: a case
806 study of Hangjinq highway, Zhuji section. *ACTA ECOLOGICA SINICA*, 34(19):5659-5669,
807 2014 (in Chinese).
- 808 Xiao, P. Q., Shi, X. J., Chen, J. N., Wu, Q., Yang, J. F., Yang, C. X., and Wang, C. G.:
809 Experimental Study on Protecting Speedway Slope Under Rainfall and Flow Scouring.
810 *Bulletin of Soil and Water Conservation*, 24(1):16-18, 2004 (in Chinese).
- 811 Xu, X. L., Liu, W., Kong, Y. P., Zhang, K. L., Yu, B. F., Chen, J. D.: Runoff and water erosion on
812 road side-slopes: Effects of rainfall characteristics and slope length. *Transportation Research*

- 813 Part D: Transport and Environment, 14(7): 497-501, 2009.
- 814 Yang, X.: Deriving rusle cover factor from time-series fractional vegetation cover for hillslope
815 erosion modelling in new south wales. *Soil Research*, 52(52): 253-261, 2014.
- 816 Yang, Y. C., Wang, M. Z., Xu, Y. Y., Wang, P. C., and Song, Z. P.: Prediction of Soil Erosion on
817 Embankment Slope of Qinhuangdao-Shenyang Special Line for Passenger Trains. *Journal of*
818 *Soil and Water Conservation*, 15(2):14-16, 2001(in Chinese).
- 819 Yang, Y., and Wang, K.: Discussions on the Side Slope Protection System For Expressway.
820 *Industrial Safety and Environmental Protection*, 32(1):47-49, 2006 (in Chinese).
- 821 Yang, Z. S.: A Study on Erosive Force of Rainfall on Sloping Cultivated Land in the Northeast
- 822 Yang, Z. S.: Study on Soil Loss Equation in Jinsha River Basin of Yunnan Province. *Journal of*
823 *mountain science*, 20: 3-11, 2002 (in Chinese).
- 824 Yang, Z. S.: Study on Soil Loss Equation of Cultivated Slopeland in Northeast Mountain Region
825 of Yunnan Province. *Bulletin of Soil and Water Conservation*, (1): 1-9, 1999 (in Chinese).
- 826 yield in Liao watershed, Jiangxi Province, China, using USLE, GIS, and RS. *Journal of Earth*
827 *Science* 2 (6), 941-953, 2010
- 828 Yoder, D. C., Foster, G. R., Renard, K. G., Weesies, G. A., and Mccool, D. K.: C-factor calculations
829 in RUSLE. American Society of Agricultural Engineers. Meeting (USA), 1993.
- 830 Yuan, C., Yu, Q. H., You, Y. H., Guo, L.: Deformation mechanism of an expressway embankment
831 in warm and high ice content permafrost regions. *Applied Thermal Engineering* 121: 1032-
832 1039, 2017.
- 833 Yuan, C., Yu, Q. H., You, Y. H., Guo, L.: Deformation mechanism of an expressway embankment
834 in warm and high ice content permafrost regions. *Applied Thermal Engineering* 121: 1032-
835 1039, 2017.
- 836 Yuan, J. P.: Preliminary Study on Grade Scale of Soil Erosion Intensity. *Bulletin of Soil and Water*
837 *Conservation*, 19(6):54-57, 1999 (in Chinese).
- 838 Zeng, C., Wang, S. J., Bai, X. Y., Li, Y. B., Tian, Y. C., Li, Y., Wu, L. H., and Luo, G. J. : Soil
839 erosion evolution and spatial correlation analysis in a typical karst geomorphology using
840 RUSLE with GIS. *Solid Earth*, 8(4), 1-26, 2017.
- 841 Zerihun, M., Mohammedyasin, M. S., Sewnet, D., Adem, A. A., & Lakew, M.: Assessment of soil
842 erosion using RUSLE, GIS and remote sensing in NW Ethiopia. *Geoderma Regional*,12: 83-
843 90, 2018.
- 844 Zerihun, M., Mohammedyasin, M. S., Sewnet, D., Adem, A. A., Lakew, M.: Assessment of soil
845 erosion using RUSLE, GIS and remote sensing in NW Ethiopia. *Geoderma Regional*, 12, 83-
846 90, 2018.
- 847 Zhang, D. S.: The calculation of urban soil erosion based on GIS-a case study of Wuhan City.
848 Southwest University of M.S.Dissertation, 2011 (in Chinese).
- 849 Zhang, H., Liao, X. L., Zhai, T. L.: Evaluation of ecosystem service based on scenario simulation
850 of land use in Yunnan Province. *Physics and Chemistry of the Earth, Parts A/B/C*. 2017.
- 851 Zhang, T., Jin, D. G., Dong, G. C., Lin, J., Tang, P., Li, L. P.: Monitoring Soil Erosion in Linear

- 852 Production and Construction Project Areas Based on RUSLE-A Case Study of North Ring
853 Expressway in Ningbo City, Zhejiang Province. *Bulletin of Soil and Water Conservation*,
854 36(5): 131-135, 2016 (in Chinese).
- 855 Zhang, T., Jin, D. G., Tong, G. C., Lin, J., Tang, P., Li, L. P.: Monitoring Soil Erosion in Linear
856 Production and Construction Project Areas Based on RUSLE - A Case Study of North Ring
857 Expressway in Ningbo City, Zhejiang Province. *Bulletin of Soil and Water Conservation*,
858 36(5):131-135, 2016 (in Chinese).
- 859 Zhao, C. C., Ding, Y. J., Ye, B. S., Zhao, Q. D.: Spatial distribution of precipitation in Tianshan
860 Mountains and its estimation. *Advance in water science*, 22:315-322, 2011 (in Chinese)
- 861 Zhao, L., Yuan, G. L., Zhang, Y., He, B., Liu, Z. H., Wang, Z. Y., Li, J.: The Amount of Soil
862 Erosion in Baoxiang Watershed of Dianchi Lake Based on GIS and USLE. *Bulletin of Soil
863 and Water Conservation*, 27(3): 42-46, 2007 (in Chinese).
- 864 Zhou, F. C.: Highway Slope Ecological Protection Against Erosion Mechanism and Control Effect
865 Research. Chongqing jiaotong university, 2010 (in Chinese).
- 866 Zhou, R. G., Zhong, L. D., Zhao, N. L., Fang, J., Chai, H., Jian, Z., Wei, L., Li. B.: The
867 Development and Practice of China Highway Capacity Research. *Transportation Research
868 Procedia*, 15: 14-25, 2016.
- 869 Zhou, R. G., Zhong, L. D., Zhao, N. L., Fang, J., Chai, H., Jian, Z., Wei, L., Li. B.: The
870 Development and Practice of China Highway Capacity Research. *Transportation Research
871 Procedia*, 15: 14-25, 2016.
- 872 Zhu, J., Li, Y. M., Jiang, D. M.: A Study on Soil Erosion in Alpine and Gorge Region Based on
873 GIS and RUSLE Model-Taking Lushui County of Yunnan Province as an Example. *Bulletin
874 of Soil and Water Conservation*, 36(3): 277-283, 2016 (in Chinese).
- 875 Zhu, S. Q., Lin, J. L., and Lin, W. L.: Preliminary Study on Effects of Expressway Construction on
876 Side-Slope Soil Erosion in Mountainous Areas. *Resources Science*, 26(1):54-60, 2004 (in
877 Chinese).
- 878 Zhuo, M. N., Li, D. Q., and Zheng, Y. J.: Study on Soil and Water Conservation Effect of
879 Bioengineering Techniques for Slope Protection in Highway. *Journal of Soil and Water
880 Conservation*, 20(1):164-167, 2006 (in Chinese).